

## Sayan–Biryusa Volcanoplutonic Belt (Southern Siberian Craton): Age and Petrogenesis

T.V. Donskaya<sup>a,✉</sup>, D.P. Gladkochub<sup>a</sup>, A.M. Mazukabzov<sup>a</sup>,  
P.A. L'vov<sup>b</sup>, E.I. Demonerova<sup>a</sup>, Z.L. Motova<sup>a</sup>

<sup>a</sup> Institute of the Earth's Crust, Siberian Branch of the Russian Academy of Sciences, ul. Lermontova 128, Irkutsk, 664033, Russia

<sup>b</sup> A.P. Karpinsky Russian Geological Research Institute, pr. Srednii 74, St. Petersburg, 199106, Russia

Received 14 June 2017; received in revised form 21 December 2017; accepted 25 April 2018

**Abstract**—Geological, geochronological, and geochemical isotope studies are carried out for metamorphosed volcanic rocks and dolerites of the Maltsevka sequence of the Elash Group in the Biryusa block of the Siberian craton. It is found that mafic igneous rocks (dolerites and basaltic andesites) are close in composition to intraplate basalts. Flat or slightly fractionated REE patterns ( $(La/Yb)_n = 1.3–2.3$ ) and positive  $\epsilon_{Nd}(T)$  values of +3.7 and +4.1 are observed. It is assumed that the depleted asthenospheric mantle and, possibly, plume mantle were the sources of these rocks, while the lithospheric mantle had no significant effect. Meta-andesites of the Maltsevka sequence belong to the tholeiitic series and have high La, Th, and U contents. Pronounced negative Nb and Ti anomalies are observed in the multielement patterns of these rocks, along with negative  $\epsilon_{Nd}(T)$  values of –4.6. It is assumed that meta-andesites were resulted from the late Archean crustal melting with the participation of the mantle material. Metarhyolites prevalent in the Maltsevka sequence are divided into two groups similar in REE composition to *A*-type and *I*-type granites. *A*-type metarhyolites show high contents of Zr, Y, Nb, Th, and REE (except for Eu) and positive  $\epsilon_{Nd}(T)$  values of +2.2 and might have resulted from the melting of the source with geochemical isotope parameters close to those of mafic igneous rocks of the Maltsevka sequence. *I*-type metarhyolites have low contents of Y, Yb, Zr, and Nb but high contents of Th and show negative  $\epsilon_{Nd}(T)$  values of –3.7. They might have resulted from the melting of lower crustal diorite–tonalite rocks with addition of juvenile mantle material to the magma generation area. U–Pb zircon dating of metarhyolites of the Maltsevka sequence corresponding to *A*- and *I*-type granites showed that they are close in age,  $1872 \pm 10$  and  $1874 \pm 10$  Ma, respectively, which agrees with the age estimated earlier for granitoids of the Sayan complex of the Biryusa block. The similar ages and structural positions, along with the localization within the same structure, made it possible to unite volcanic rocks of the Elash Group and granitoids of the Sayan complex of the Biryusa block into a Paleoproterozoic volcanoplutonic association. The rocks of the association form the Sayan–Biryusa volcanoplutonic belt stretching for about 300 km along the zone of junction of the Biryusa block of the Angara fold belt and the Archean Tunguska superterrane of the Siberian craton. The belt is part of the large Paleoproterozoic South Siberian postcollisional magmatic belt formed at the final formation stage of the Siberian craton, when it was possibly part of the Paleoproterozoic Columbia supercontinent.

**Keywords:** volcanic rocks, U–Pb zircon age, geochemistry, Nd isotope data, Paleoproterozoic, Siberian craton

### INTRODUCTION

Volcanoplutonic belts are crustal structures formed as a result of a single stage of endogenic activity and composed of volcanic and intrusive rocks of a similar age. Currently, there are two Paleoproterozoic volcanoplutonic belts identified and well researched in the Siberian craton area. One of them, the North Baikal belt, is a part of the South Siberian postcollisional magmatic belt (Fig. 1). It was formed at the postcollisional extension stage, which followed the establishment of the Siberian craton structure (Larin et al., 2003). The rocks of the belt aged 1.87–1.85 Ga are represented by volcanoterrigenous rocks of the Akitkan Group and granitoids attributed to the Irel complex (Neimark et al., 1991,

1998; Larin et al., 2003; Donskaya et al., 2005, 2008). The second one, i.e., the younger Bilyakchan–Ulkan belt, which intersects the rocks at the east of the Aldan and Stanovoi provinces (Fig. 1), was formed at the anorogenic stage of the Siberian craton evolution. The rocks of the belt include volcanosedimentary deposits of the Bilyakchan and Ulkan Groups, as well as magmatic rocks of the Ulkan–Dzhugdzhur association aged 1.74–1.70 Ga (Nemark et al., 1992; Larin et al., 1997, 2012; Didenko et al., 2010; Larin, 2011, 2014).

The third one, the Paleoproterozoic Sayan–Biryusa volcanoplutonic belt was identified in the Prisayan marginal basement uplift in the south of the Siberian craton (the Biryusa block) as a result of thorough geological, geochronological, and geochemical isotope studies of volcanic rocks of the Maltsevka sequence of the Elash Group and comparison of the data obtained with published research results on

✉ Corresponding author.

E-mail address: tanlen@crust.irk.ru (T.V. Donskaya)

Paleoproterozoic granitoids of the Sayan complex. Similarly to the North Baikal belt, the Sayan–Biryusa volcanoplutonic belt is a part of South Siberian postcollisional magmatic belt, and studying the formation details of its intrusive and effusive rocks is a very topical problem, since volcanoplutonic associations are formed rather rarely in postcollisional geodynamic settings. The results of petrographic, geochronological, geochemical, and isotope studies of volcanic rocks of the Maltsevka sequence of the Sayan–Biryusa volcanoplutonic belt are presented in the paper, and possible causes for different compositions of igneous rocks formed within the same volcanoplutonic belt are considered.

### GEOLOGICAL POSITION OF THE MALTSEVKA SEQUENCE OF THE ELASH GROUP OF THE BIRYUSA BLOCK

The Biryusa block is located in the southwest of the Siberian craton within the Prisan marginal uplift. According to the tectonic scheme produced by O.M. Rosen (2003), the rocks of the block belong to the Angara fold belt (Fig. 1). The Biryusa block is composed of late Archean rocks of the Khailama and Monkress Groups overlapped by Paleoproterozoic rocks of the Elash and Neroi Groups (Fig. 2) (Belichenko, 1988; Turkina et al., 2006; Dmitrieva and Nozhkin, 2012). In addition, granitoids of the Sayan complex aged 1.90–1.86 Ga are rather common in the Biryusa block (Fig. 2) (Levitskii et al., 2002; Turkina et al., 2003, 2006; Donskaya et al., 2014; Makagon et al., 2015). These granitoids intrude the Archean rocks of the Khailama and Monkress Groups and Paleoproterozoic rocks of the Elash Group and contact with late Paleoproterozoic rocks of the Neroi Group along the tectonic zones (Belichenko, 1988; Dmitrieva and Nozhkin, 2012; Donskaya et al., 2014; Nozhkin et al., 2015). Compositions of Paleoproterozoic granitoids of the Sayan complex are rather diverse, as they include *I*-type tonalites and diorites (Turkina, 2005; Turkina et al., 2006; Makagon et al., 2015), two-mica *S*-type granites (Donskaya et al., 2014) and biotite-amphibolic *A*-type granites (Levitskii et al., 2002; Turkina et al., 2006; Makagon et al., 2015).

Until recently, the Elash Group has been one of the most understudied stratigraphic units of the Biryusa block. The rocks of the Elash Group fill the Elash graben overlaying the Archean rocks and unite volcanoterrigenous rocks of the Chasovenskaya and Maltsevka sequences (Fig. 3) (Galimova et al., 2012). Chasovenskaya and Maltsevka sequences are tectonically related, their relative stratigraphic positions only being identified based on the indirect data (Galimova et al., 2012). The rocks of the Elash Group are considered Paleoproterozoic, since they overlay Archean rocks and are intruded by granitoids of the Sayan complex. The lower Chasovenskaya sequence is formed by metasediments, schists with various compositions, iron formation, and amphibolites over basaltoids (Galimova et al., 2012). The upper Maltsevka sequence is formed by metaterrigenous rocks,

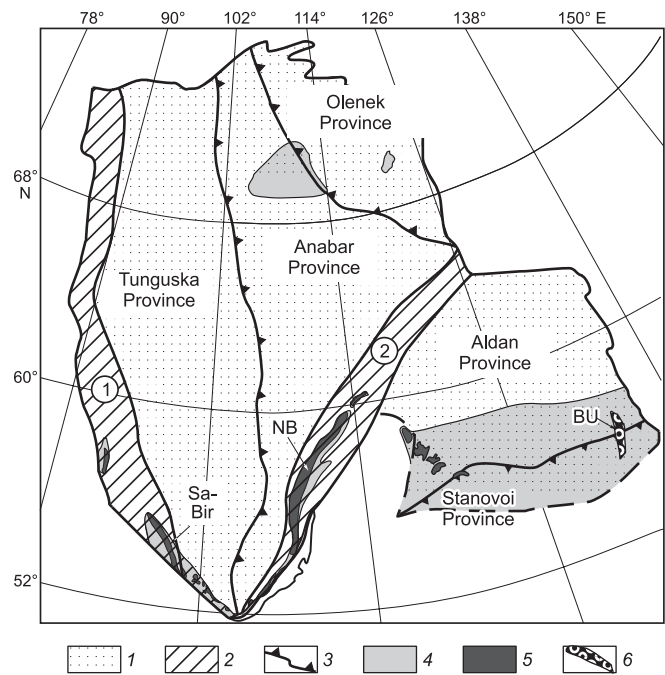


**Fig. 1.** Main tectonic elements of the Siberian craton and location of the South Siberian postcollisional magmatic belt (modified from (Rozen, 2003; Larin et al., 2003; Gladkochub et al., 2006)). 1, main provinces (superterrane); 2, Paleoproterozoic fold belts; 3, suture zones; 4, basement uplifts; 5, outcrops of Paleoproterozoic rocks of the South Siberian postcollisional magmatic belt; 6, outcrops of late Paleoproterozoic rocks of the Bilyakchan–Ulkan volcanoplutonic belt. Numbers in circles read as follows: 1, Angara fold belt; 2, Akitkan fold belt. Letters read as follows: BU, Bilyakchan–Ulkan volcanoplutonic belt; Sa-Bir, Sayan–Biryusa volcanoplutonic belt; NB, North Baikal volcanoplutonic belt.

tuffs, and volcanic rocks with various compositions (Galimova et al., 2012). Terrigenous rocks of the Maltsevka sequence include metasediments, metasiltstones, and schists with various compositions, while volcanic rocks include basaltic andesites, andesites, dacites, and rhyolites with prevalence of felsic volcanic rocks. Volcanic rocks account for the major part of sections (up to 90%) in some areas. In addition, subvolcanic facies rocks including metadolerites, metagabbro-dolerites, granite-porphyr, rhyolites, and dacites are identified in the Maltsevka sequence (Galimova et al., 2012).

### GEOLOGICAL AND PETROGRAPHIC CHARACTERISTICS OF THE MAIN RESEARCH OBJECTS

Thorough studies rocks of the Maltsevka sequence of the Elash Group were carried out in two sites, one in the Tagul river basin (hereinafter Tagul site) and one in its tributary Toporok River (hereinafter Toporok site). Here, volcanic rocks are prevalent in the section, and intervals between them are composed of metaterrigenous rocks and tuffs (Fig. 3).

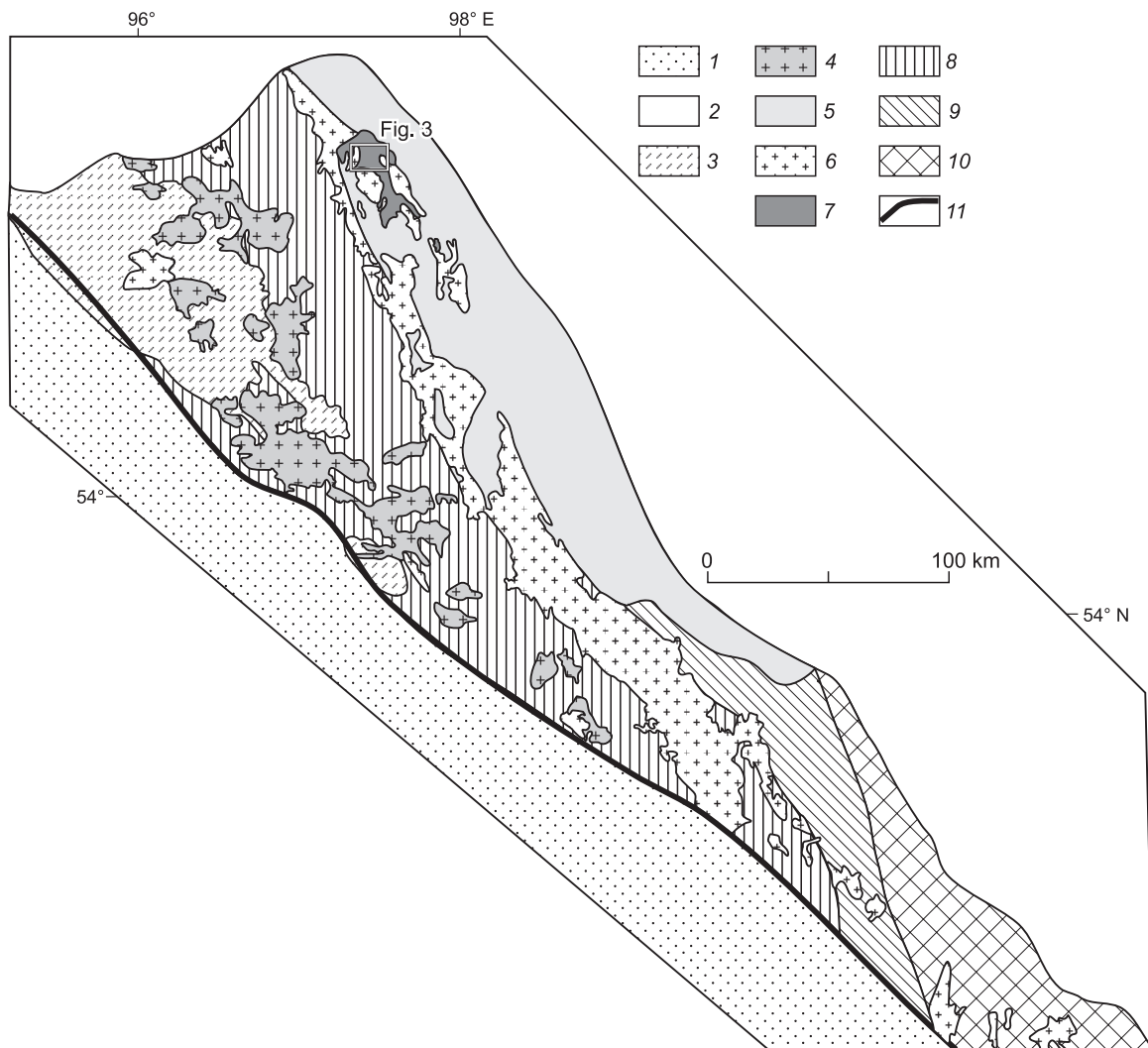


**Fig. 2.** Geological structure of the Biryusa block of the Prisayan basement uplift of the Siberian craton (modified from (Yanshin, 1983; Donskaya et al., 2014)). 1, Central Asian fold belt; 2, Phanerozoic rocks of the Siberian Platform cover; 3, Devonian volcanosedimentary rocks of overlapping troughs; 4, Paleozoic granitoids; 5, Vendian-late Riphean sedimentary rocks; 6, Paleoproterozoic granitoids of the Sayan complex; 7, Paleoproterozoic volcanoterrigenous rocks of the Elash Group; 8, Paleoproterozoic-late Archean rocks of the Biryusa block (undivided); 9, Paleoproterozoic rocks of the Urik-Iya terrane; 10, Archean rocks of the Sharyzhalgai basement uplift; 11, Main Sayan Fault.

Bedrock outcrops in the Tagul site (Fig. 3) primarily reveals gray-green metavolcanic rocks with small metamorphosed dolerite bodies.

Felsic metavolcanic rocks of the Tagul site are metamorphosed rocks with porphyric texture. Porphyry impregnations are represented by relict phenocrysts of partially sericitized plagioclase. The groundmass mostly consists of quartz and feldspar, which in some areas display a relict felsite texture, as well as sericite, chloritized biotite, and epidote. Newly formed quartz porphyroblasts are observed in some areas. In addition, quartz may form secondary veinlets sometimes in combination with albite, chlorite, and epidote. Accessory minerals are represented by zircon, sphene, orthite, and ore mineral.

Metamorphosed dolerites (mafic subvolcanic rocks) are characterized by cataclastic and granoblastic textures, as

well as by relict porphyric, microdolerite, and intersertal textures. Relict porphyric phenocrysts are represented by plagioclase laths, while the groundmass is formed mostly by fine-grained plagioclase aggregate, as well as larger hornblende aggregates, which possibly replace clinopyroxene, and actinolite. Chlorite partially develops over hornblende. Metamorphosed dolerites include ore mineral as a secondary mineral with its content reaching 5%.

Bedrock outcrops in the Toporok site (Fig. 3) reveal the alteration of gray-green, gray, and light gray metavolcanic rocks with various compositions with small metamorphosed dolerite bodies. Intermediate-mafic and felsic volcanic rocks are observed within isolated sites, i.e., alteration of intermediate-mafic and felsic volcanic rocks was not observed within the same outcrop.

Felsic metavolcanic rocks of the Toporok site are altered to various degrees and display lepidogranoblastic, porphyroblastic, and cataclastic textures, which, however, include preserved areas of relict porphyric and felsite textures. Porphyric phenocrysts are represented by relict sericitized plagioclase. The felsic metavolcanic rock groundmass consists mostly of a quartz-feldspar aggregate, sericite, and biotite replaced mostly by chlorite. Individual varieties show a unidirectional localization of scaly minerals, which determines the schistose character of these rocks. In addition, porphyroblastic structures of newly formed quartz are observed in metavolcanic rocks. Accessory minerals are represented by zircon, tourmaline, and rutile.

Mafic metavolcanic rocks mostly consist of fine-grained lepidogranoblastic quartz-feldspar groundmass with nonuniformly distributed chlorite and ore mineral. Occasionally, the structures are similar to relict porphyric plagioclase bodies. In addition, newly formed biotite porphyroblasts are observed in the rocks.

Mafic metavolcanic (basaltic andesite) rocks are metamorphosed rocks with lepidoblastic texture with areas of preserved relict pilotaxitic and porphyric textures. Porphyry phenocrysts are represented by saussuritized plagioclase laths. The groundmass mostly consists of plagioclase, amphibole (actinolite), chlorite, biotite, and ore mineral.

Metamorphosed dolerites (mafic subvolcanic rocks) of the Toporok site are similar to metadoleresites of the Tagul site, apart from areas with intense manifestations of plagioclase saussurization.

## METHODS

Nineteen samples of metamorphosed volcanic rocks and three samples of metadoleresites from the Maltsevka sequence were analyzed for contents of major, trace, and rare-earth elements. Sm–Nd isotope analysis was performed for five samples. U–Th–Pb zircon dating was carried out for two samples of felsic volcanic rocks. Sample points for geochemical, isotope, and geochronological studies are shown in Fig. 3.

Contents of major elements were determined via silicate analysis at the Center Geodynamics and Geochronology of the Institute of the Earth's Crust SB RAS (analysts M.M. Samoilenko and N.Yu. Tsareva). Contents of rare and rare-earth elements were determined by ICP-MS method at the Ultramicroanalysis common use center of the Limnological Institute SB RAS using an Agilent 7500ce quadrupole mass spectrometer (Agilent Technologies Inc., the USA) (analyst S.V. Panteeva). Element concentrations in samples were calculated with reference to G-2 and GSP-2 international standards. Chemical decomposition of the samples for ICP-MS analysis was performed at the Center for Geodynamics and Geochronology of the Institute of the Earth's Crust SB RAS via lithium metaborate melting using the technique described in (Panteeva et al., 2003), which made it possible to

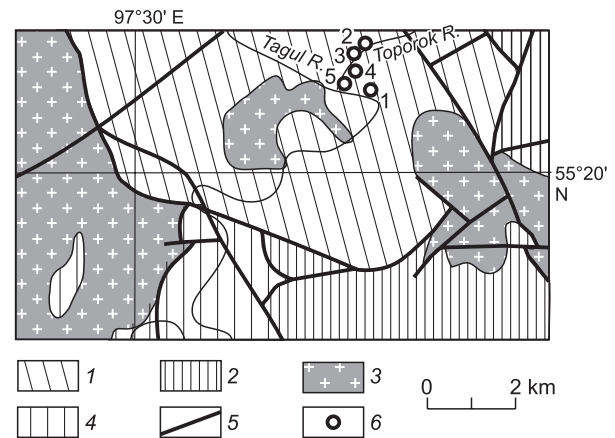


**Fig. 3.** Geological structure of the middle Tagul site. 1, Paleoproterozoic volcanoterrigenous rocks of the Maltsevka sequence of the Elash Group; 2, Paleoproterozoic volcanoterrigenous rocks of the Chasovensskaya sequence of the Elash Group; 3, Paleoproterozoic granitoids of the Sayan complex; 4, late Archean (?) rocks of the Biryusa block (undivided); 5, main faults; 6, sample points (1, Tagul site, sample Nos. 1526, 1527, 1528; 2–5, Toporok site: 2, sample Nos. 1512, 1513, 1514, 1515, 1516, 1517, 3, sample nos 1518, 1519, 1520, 1521, 1522, 1523, 4, sample Nos. 1524, 1540, 1541, 1542, 1543, 1544, 5, sample No. 1525).

achieve complete dissolution of all minerals. Errors in ICP-MS measurements of trace and rare-earth element contents did not exceed 5%.

Sm–Nd isotope analysis was carried out at the Institute of the Earth's Crust SB RAS. Volcanic rock samples in the form of thinly grated powders were consecutively treated with 2M HCl solution and ultrapure water (ELGA purification system) before chemical sample preparation to remove secondary mineral phases. The processed 100 mg samples were dried, and a  $^{149}\text{Sm}$ – $^{150}\text{Nd}$  tracer solution was added. Chemical decomposition was performed in a  $\text{HNO}_3$ – $\text{HF}$ – $\text{HClO}_4$  concentrated acid mixture at the temperature of about 140–160 °C until their complete dissolution. The aggregate of rare-earth elements was isolated in columns filled with 2 ml BioRed AG 50W×8 resin. Further Sm isotope separation from Nd was performed in columns filled with LnSpec resin using the technique described in (Pin and Zalduogui, 1997). Static modes of Nd and Sm isotope ratios were obtained using the Finnigan MAT-262 multicollector mass spectrometer at the Center for Geodynamics and Geochronology of the Institute of the Earth's Crust SB RAS.  $^{143}\text{Nd}/^{144}\text{Nd}$  measurements were normalized by the  $^{146}\text{Nd}/^{144}\text{Nd} = 0.7219$ . Measurement accuracy for Sm and Nd concentrations was 0.5%,  $^{147}\text{Sm}/^{144}\text{Nd}$  isotope ratio 0.5%, and for  $^{143}\text{Nd}/^{144}\text{Nd}$  0.005% ( $2\sigma$ ). The average weighted  $^{143}\text{Nd}/^{144}\text{Nd}$  value under the JNd-1 standard for the measurement period of the data published was  $0.512097 \pm 0.000013$  ( $2\sigma$ ,  $n = 8$ ). Model isotopic ages  $T_{\text{Nd}}(\text{DM})$  and  $\varepsilon_{\text{Nd}}(T)$  values were measured using the up-to-date values for the chondrite uniform reservoir CHUR from (Jacobsen and Wasserburg, 1984) and depleted mantle DM from (Goldstein and Jacobsen, 1988).

Zircon was isolated from felsic metavolcanic rock samples (Nos. 1527 and 1540) via the standard technique with the use of heavy liquids. Its morphological features were studied using the CamScan MX2500S scanning electron microscope in secondary electron and cathodoluminescence modes (Centre of Isotopic Research of the Russian Geological Research Institute). U–Th–Pb zircon dating was performed using the SHRIMP-II secondary ion mass spectrometer at the Centre of Isotopic Research of the Russian Geological Research Institute. Manually selected zircon grains were implanted into the epoxy resin along with standard TEMORA zircon grains, then the prepared sample was polished, and gold sputtering was performed. U–Pb isotope ratios were measured by SHRIMP-II using the technique described in (Williams, 1998). The data obtained were processed using the SQUID software suite (Ludwig, 2000). U–Pb isotope ratios were normalized by 0.0665, which is the value attributed to the standard TEMORA zircon corresponding to the zircon age of 416.75 Ma (Black et al., 2003). Concordance plots were constructed using the ISOPLOT/EX software suite (Ludwig, 1999). Individual analyses (of isotope ratios and ages) were carried out with 1 sigma error, and concordance age calculations are presented with 2 sigma error.

## U–Th–Pb GEOCHRONOLOGY RESULTS

Metamorphosed felsic volcanic rock sample no. 1527 was collected in the Tagul site (55°21.042' N, 97°34.822' E). The sample point is shown in Fig. 3. Accessory zircon in the form of colorless and sometimes smoky transparent idiomorphic crystals was isolated from the sample. Zircon grain size varied from 150 to 250 μm with crystal elongations of 1:2 and 1:3. Cathodoluminescent images of zircon display magmatic zoning (Fig. 4a). Results for ten zircon grains are presented in Table 1 and Fig. 4b. Uranium and thorium concentrations in the grains analyzed are 152–488 ppm and 73–273 ppm, respectively. <sup>232</sup>Th/<sup>238</sup>U isotope ratios vary within the narrow range of 0.43 to 0.58. In U–Pb isotope concordance plot (Fig. 4b), nine isotopic composition points for the zircon analyzed are located in its concordance line, while zircon concordance age is 1872 ± 10 Ma (with mean square weighted deviation (MSWD) of 0.043). Isotopic composition point No. 10.1 was excluded from concordance age calculations due to discordance of the values obtained (Table 1). Given the morphological features of zircon, which imply its magmatic origin, the age of 1872 ± 10 Ma may be interpreted as the estimate of zircon crystallization age and

**Table 1.** U–Pb zircon dating results for metarhyolites of the Maltsevka sequence of the Elash Group

Sample, crystal, crater	<sup>206</sup> Pb <sub>c</sub> , %	U, ppm	Th, ppm	<sup>232</sup> Th/ <sup>238</sup> U	<sup>206</sup> Pb*, ppm	Isotopic ratios								<i>Rho</i>	Age, Ma		<i>D</i> , %
						<sup>238</sup> U/ <sup>206</sup> Pb*		<sup>207</sup> Pb*/ <sup>206</sup> Pb*		<sup>207</sup> Pb*/ <sup>235</sup> U		<sup>206</sup> Pb*/ <sup>238</sup> U*			<sup>206</sup> Pb/ <sup>238</sup> U	<sup>207</sup> Pb/ <sup>206</sup> Pb	
						(1)	±%	(1)	±%	(1)	±%	(1)	±%				
Metarhyolites of the Tagul site (sample No. 1527)																	
1527_1.1	0.15	488	273	0.58	147.0	2.862	1.4	0.1143	0.72	5.502	1.5	0.3492	1.4	0.886	1931 ± 23	1868 ± 13	–3
1527_2.1	0.31	208	87	0.43	59.7	3.003	1.4	0.1157	1.50	5.310	2.1	0.3328	1.4	0.685	1852 ± 23	1891 ± 27	2
1527_3.1	0.21	274	123	0.46	79.1	2.988	1.4	0.1141	0.95	5.260	1.7	0.3345	1.4	0.828	1860 ± 23	1865 ± 17	0
1527_4.1	0.38	236	105	0.46	69.7	2.914	1.5	0.1141	1.40	5.400	2.0	0.3428	1.5	0.716	1900 ± 24	1866 ± 26	–2
1527_5.1	0.24	279	146	0.54	79.8	3.010	1.4	0.1150	1.00	5.264	1.8	0.3320	1.4	0.809	1848 ± 23	1880 ± 19	2
1527_6.1	0.38	295	151	0.53	86.2	2.952	1.4	0.1146	1.40	5.350	2.0	0.3385	1.4	0.725	1879 ± 23	1874 ± 24	0
1527_7.1	0.63	152	73	0.50	43.9	2.991	1.5	0.1136	1.80	5.230	2.3	0.3339	1.5	0.635	1857 ± 24	1858 ± 33	0
1527_8.1	0.38	254	116	0.47	75.3	2.904	1.9	0.1151	1.10	5.460	2.2	0.3440	1.9	0.861	1906 ± 31	1882 ± 20	–1
1527_9.1	0.09	330	178	0.56	94.4	3.001	1.4	0.1137	0.93	5.222	1.7	0.3332	1.4	0.835	1854 ± 23	1859 ± 17	0
1527_10.1	0.20	297	154	0.54	92.7	2.758	1.4	0.1150	1.10	5.740	1.8	0.3624	1.4	0.798	1993 ± 25	1879 ± 20	–6
Metarhyolites of the Toporok site (sample No. 1540)																	
1540_1.1	0.22	555	202	0.38	159.0	3.004	1.3	0.1146	0.79	5.259	1.5	0.3328	1.3	0.859	1852 ± 21	1874 ± 14	1
1540_2.1	0.15	440	170	0.40	127.0	2.982	1.3	0.1145	0.68	5.293	1.5	0.3352	1.3	0.892	1863 ± 22	1872 ± 12	0
1540_3.1	1.29	250	106	0.44	70.2.0	3.097	1.4	0.1200	1.50	5.330	2.0	0.3221	1.4	0.691	1800 ± 22	1956 ± 26	9
1540_4.1	0.29	748	497	0.69	220.0	2.925	1.3	0.1139	0.67	5.364	1.5	0.3417	1.3	0.895	1895 ± 22	1862 ± 12	–2
1540_5.1	1.04	271	117	0.45	79.7	2.948	1.7	0.1146	1.50	5.350	2.3	0.3385	1.7	0.737	1879 ± 27	1873 ± 28	0
1540_6.1	0.51	434	196	0.47	130.0	2.889	1.4	0.1138	0.91	5.422	1.7	0.3457	1.4	0.832	1914 ± 23	1860 ± 17	–3
1540_7.1	0.55	441	353	0.83	126.0	3.020	1.4	0.1155	0.97	5.269	1.7	0.3308	1.4	0.816	1842 ± 22	1888 ± 18	3
1540_8.1	0.57	404	361	0.92	116.0	3.020	1.4	0.1162	1.40	5.300	2.0	0.3307	1.4	0.704	1842 ± 22	1898 ± 25	3
1540_9.1	0.58	633	253	0.41	187.0	2.925	1.3	0.1152	0.86	5.422	1.6	0.3415	1.3	0.841	1894 ± 22	1882 ± 15	–1
1540_10.1	0.25	492	277	0.58	143.0	2.957	1.3	0.1167	1.20	5.437	1.8	0.3380	1.3	0.741	1877 ± 22	1906 ± 22	2

Note. 1σ errors are used. Reference calibration error is 0.53%. Pb<sub>c</sub> and Pb\* are normal and radiogenic lead respectively. (1), normal lead correction based on <sup>204</sup>Pb measurement is introduced. *Rho* is the correlation ratio of <sup>206</sup>Pb/<sup>238</sup>U and <sup>207</sup>Pb/<sup>235</sup>U isotope ratio calculation error, *D* is the discordance.

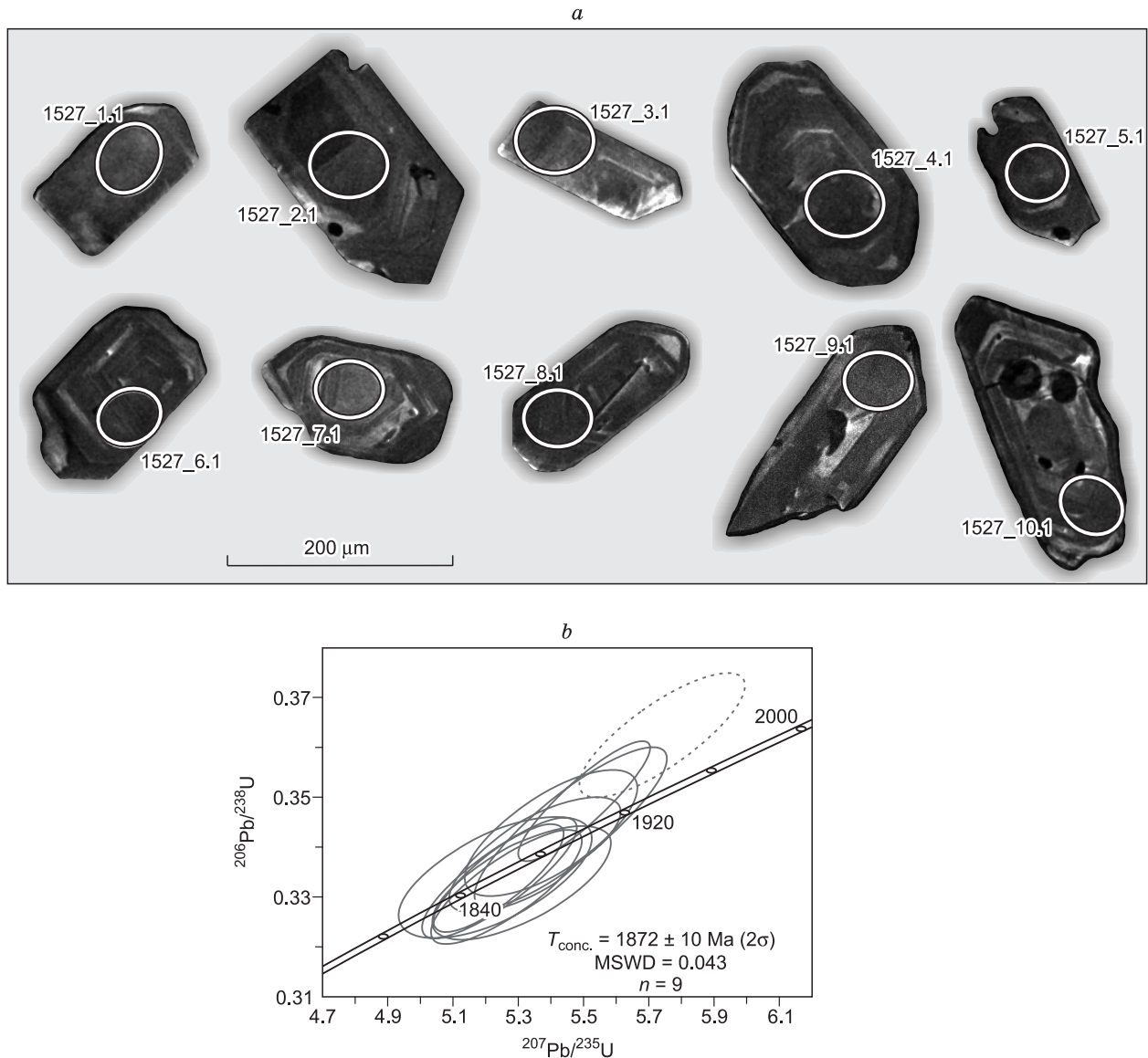


**Fig. 4.** Cathodoluminescent images of zircon crystals (a) and U–Pb dating concordance plot (b) for zircons from metamorphosed acid volcanic rock of the Maltsevka sequence of the Elash Group (Tagul site, sample No. 1527). The dotted line indicates the isotopic composition point excluded from the concordant age calculation.

thus the age of felsic volcanic rocks of the Maltsevka sequence in the Tagul site.

The second metamorphosed acid volcanic rock sample (no. 1540) was collected in the Toporok site ( $55^{\circ}21,317' \text{ N}$ ,  $97^{\circ}34,783' \text{ E}$ ). Accessory zircon is isolated from this sample in the form of honey-yellowish, transparent, oblong-prismatic, idiomorphic crystals. Zircon grain sizes varied from 120 to 300 μm, while crystal elongations varied between 1:2 and 1:4. Pronounced magmatic zoning is typical for the inner structure of zircon crystals (Fig. 5a). The analysis results for ten zircon grains are presented in Table 1 and Fig. 5b. The grains analyzed display uranium and thorium contents varying within ranges of 250–748 ppm and 106–497 ppm

respectively, as well as  $^{232}\text{Th}/^{238}\text{U}$  isotope ratio values of 0.38–0.92 (Table 1). In U–Pb isotopic concordance plot (Fig. 5b), nine isotope composition points for the zircon analyzed are located on the concordia line, while the concordance age is  $1874 \pm 10 \text{ Ma}$  (with MSWD of 0.064). Isotope composition point no. 3.1 corresponding to the zircon grain with minimum U and Th concentrations and with maximum  $^{206}\text{Pb}$  content was excluded from concordance age calculation due to discordance of the values obtained. Given the morphological features of zircon, which imply its magmatic origin, the age of  $1874 \pm 10 \text{ Ma}$  may be interpreted as the estimate of zircon crystallization age and thus the age of felsic volcanic rocks of the Maltsevka sequence in the Toporok site.

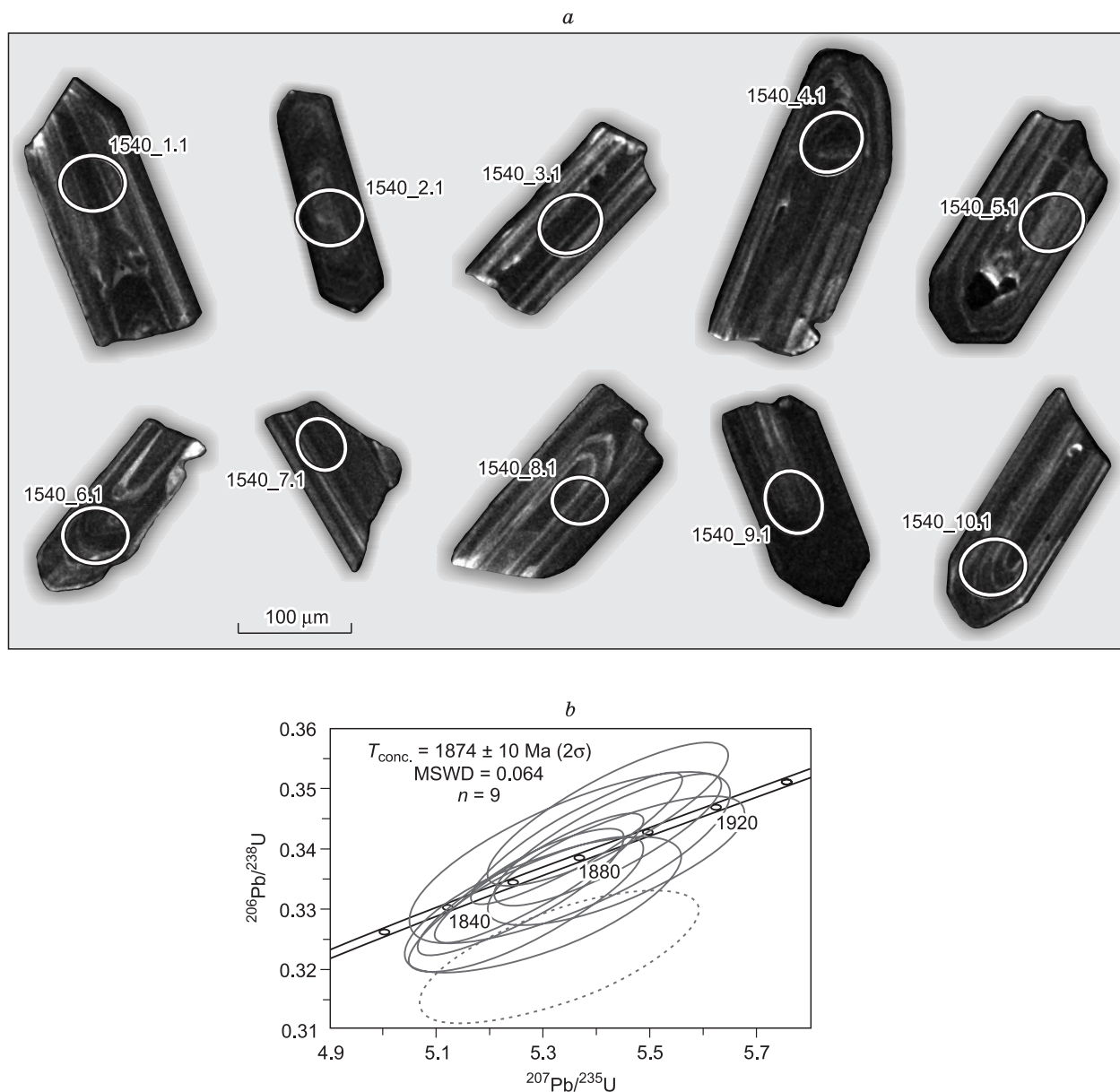


**Fig. 5.** Cathodoluminescent images of zircon crystals (*a*) and U–Pb dating concordance plot (*b*) for zircons from metamorphosed felsic volcanic rock of the Maltsevka sequence of the Elash Group (Toporok site, sample No. 1540). The dashed line indicates the isotopic composition point excluded from the concordant age calculation.

### GEOCHEMICAL CHARACTERISTICS OF IGNEOUS ROCKS OF THE MALTSEVKA SEQUENCE

Igneous rocks of the Maltsevka sequence (volcanic rocks and dolerites) are altered to various degrees as a result of metamorphic transformations in conditions of the greenschist and epidote-amphibolitic facies. In addition, small veinlets consisting of newly formed minerals are observed in these rocks. Thus, several plots, including the ones most suitable for analyzing altered rocks, were used for reliable classification of metamorphosed volcanic rocks and doler-

ites (Jensen, 1976; Winchester and Floyd, 1977). Composition points of metadolerites in the Toporok site on the classical TAS plot (Sharpenok et al., 2008) fall into the basaltic andesite field, while metadolerites in the Tagul site fall into the basalt field; imaging points for metavolcanic rocks with various compositions in the Toporok site are mostly located in andesite and rhyolite fields, the latter matching with both normal-alkaline and low-alkaline series, whereas composition points of felsic volcanic rocks in the Tagul site fall into the normal-alkaline rhyolite field (Fig. 6a). However, it should be noted that metavolcanic rocks in the Toporok site with SiO<sub>2</sub> content of 57.7 wt.% (Fig. 6a, Table 2) and quartz

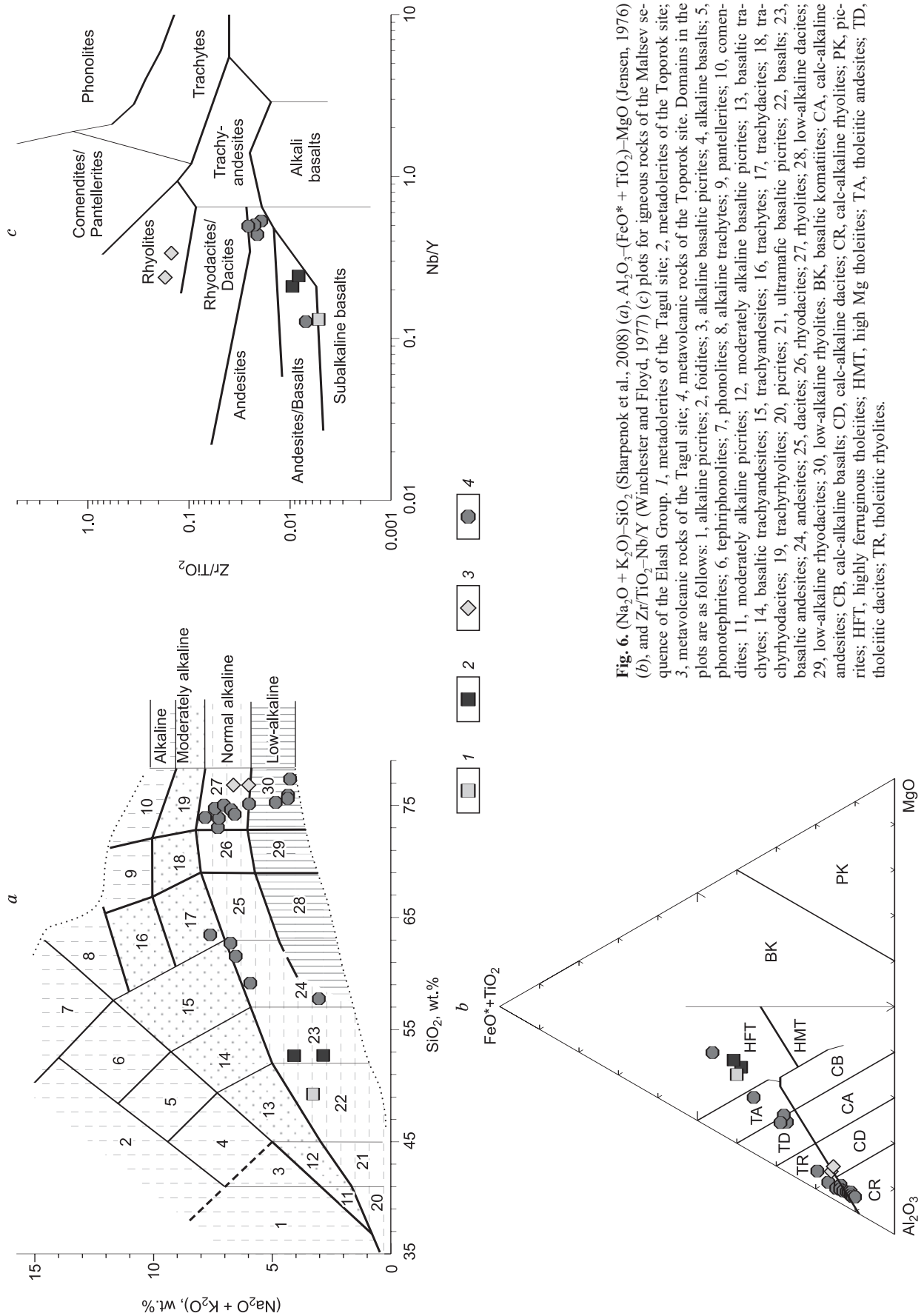


**Fig. 6.** (Na<sub>2</sub>O + K<sub>2</sub>O)–SiO<sub>2</sub> (Sharpenok et al., 2008) (a), Al<sub>2</sub>O<sub>3</sub>–(FeO\* + TiO<sub>2</sub>)–MgO (Jensen, 1976) (b), and Zr/TiO<sub>2</sub>–Nb/Y (Winchester and Floyd, 1977) (c) plots for igneous rocks of the Maltsev sequence of the Elash Group. 1, metadolерites of the Tagul site; 2, metadolерites of the Toporok site; 3, metavolcanic rocks of the Tagul site; 4, metavolcanic rocks of the Toporok site. Domains in the plots are as follows: 1, alkaline picrites; 2, foidites; 3, alkaline basaltic picrites; 4, alkaline basalts; 5, phonotephrites; 6, tephriphonolites; 7, phonolites; 8, alkaline trachytes; 9, pantellerites; 10, comendites; 11, moderately alkaline picrites; 12, moderately alkaline basaltic picrites; 13, basaltic trachytes; 14, basaltic trachyandesites; 15, trachyandesites; 16, trachytes; 17, trachydacites; 18, trachyhyodacites; 19, trachyhyolites; 20, picrites; 21, ultramafic basaltic picrites; 22, basalts; 23, basaltic andesites; 24, andesites; 25, dacites; 26, rhyodacites; 27, rhyolites; 28, low-alkaline dacites; 29, low-alkaline rhyodacites; 30, low-alkaline rhyolites. BK, basaltic komatiites; CA, calc-alkaline andesites; CB, calc-alkaline basalts; CD, calc-alkaline dacites; CR, calc-alkaline rhyolites; PK, picrites; HFT, highly ferruginous tholeiites; HMT, high Mg tholeiites; TA, tholeiitic andesites; TD, tholeiitic dacites; TR, tholeiitic rhyolites.

**Table 2.** Chemical compositions of basic and intermediate igneous rocks of the Maltsevka sequence of the Elash Group

Components	Tagul site		Toporok site					
	Metadolerite	Metadolerites		Basaltic meta-andesites	Meta-andesites			
	1528	1514	1517	1525	1512	1513	1515	1516
SiO <sub>2</sub> , wt.%	49.25	52.71	52.75	57.73	62.75	61.57	63.42	59.11
TiO <sub>2</sub>	2.15	1.17	1.22	2.25	0.52	0.55	0.58	0.43
Al <sub>2</sub> O <sub>3</sub>	16.77	14.98	14.04	11.21	16.76	17.21	16.64	15.81
Fe <sub>2</sub> O <sub>3</sub>	1.90	2.25	2.60	1.25	1.17	1.20	1.53	1.68
FeO	10.48	9.63	9.96	10.08	5.70	6.27	5.75	8.66
MnO	0.20	0.25	0.23	0.28	0.06	0.06	0.06	0.21
MgO	4.78	5.21	5.45	4.40	2.49	2.95	2.29	3.11
CaO	10.01	8.03	8.99	7.88	2.13	1.14	1.09	2.02
Na <sub>2</sub> O	2.93	3.47	2.55	1.69	4.14	5.69	5.40	2.27
K <sub>2</sub> O	0.31	0.62	0.31	1.31	2.59	0.80	2.17	3.58
P <sub>2</sub> O <sub>5</sub>	0.22	0.17	0.19	0.25	0.12	0.27	0.09	0.07
LOI	1.34	1.62	1.30	1.74	1.53	2.20	1.34	3.02
H <sub>2</sub> O <sup>-</sup>	0.04	0.09	0.21	0.06	0.17	0.15	0.07	0.27
CO <sub>2</sub>	<0.06	<0.06	0.08	<0.06	0.11	0.13	<0.06	0.07
Total	100.38	100.20	99.87	100.14	100.24	100.19	100.43	100.30
Rb, ppm	5	17	9	57	95	27	107	148
Sr	147	135	124	93	78	87	83	81
Y	36	23	31	48	28	32	25	24
Zr	105	97	115	159	114	114	112	108
Nb	5	6	7	6	14	14	13	12
Ba	52	124	73	211	575	300	1323	640
La	7.17	7.76	11.31	8.64	42.22	38.66	29.27	28.98
Ce	18.96	17.34	24.60	22.11	86.01	81.27	57.06	54.06
Pr	2.82	2.32	3.07	3.41	9.92	9.57	6.86	6.46
Nd	14.13	10.25	13.06	17.22	36.19	35.00	25.32	23.70
Sm	4.49	2.79	3.65	5.79	7.07	6.95	4.98	2.79
Eu	1.11	0.77	0.87	1.30	1.22	1.06	0.75	0.94
Gd	4.17	2.87	3.12	5.24	4.61	4.59	3.38	2.93
Tb	0.78	0.52	0.58	0.99	0.73	0.75	0.56	0.49
Dy	5.44	3.81	4.32	6.97	4.74	4.83	3.88	3.39
Ho	1.25	0.86	1.06	1.59	1.01	1.08	0.86	0.81
Er	3.68	2.43	3.18	4.51	2.91	3.06	2.55	2.47
Tm	0.57	0.38	0.49	0.68	0.44	0.46	0.39	0.38
Yb	3.40	2.37	3.18	4.14	2.65	2.88	2.33	2.38
Lu	0.59	0.42	0.52	0.72	0.46	0.48	0.39	0.40
Hf	3.00	2.54	3.16	4.60	3.60	3.39	3.42	3.15
Ta	0.35	0.38	0.45	0.52	1.24	1.26	1.16	1.04
Th	0.57	1.39	1.73	1.13	17.38	16.44	15.80	14.14
U	0.28	0.77	0.82	0.85	4.25	4.46	3.65	3.49
Mg#	45	48	48	45	44	46	40	39
(La/Yb) <sub>n</sub>	1.36	2.12	2.30	1.35	10.33	8.67	8.11	7.87
(La/Sm) <sub>n</sub>	0.91	1.59	1.78	0.86	3.43	3.19	3.37	5.96
Eu/Eu*	0.79	0.84	0.79	0.73	0.66	0.58	0.56	1.01
(Nb/La) <sub>PM</sub>	0.64	0.70	0.56	0.68	0.32	0.35	0.43	0.39
Nb/Nb*	0.80	0.58	0.51	0.66	0.18	0.19	0.21	0.20
(Th/La) <sub>PM</sub>	0.65	1.45	1.24	1.06	3.33	3.44	4.36	3.94

Note. Mg# =  $Mg \cdot 100 / (Mg + Fe^{2+})$ , where  $Mg = MgO/40.31$ ,  $Fe^{2+} = (Fe_2O_3^* \times 0.8998 \times 0.85) / 71.85$ ;  $Eu/Eu^* = Eu_n / (\sqrt{(Sm_n \times Gd_n)})$ ,  $Nb/Nb^* = Nb_{PM} / (\sqrt{(Th_{PM} \times La_{PM})})$ .

*n*, Chondrite-normalized values (Wakita et al., 1970); PM, primitive mantle normalized values (Sun and McDonough, 1989).

**Table 3.** Chemical compositions of metarhyolites of the Maltsevka sequence of the Elash Group

Components	Tagul site		Toporok site											
	1526	1527	1518	1519	1520	1521	1522	1523	1524	1540	1541	1542	1543	1544
SiO <sub>2</sub> , wt.%	76.81	76.77	72.96	74.44	74.96	75.08	73.88	75.18	77.27	74.16	73.83	74.68	75.56	75.81
TiO <sub>2</sub>	0.18	0.14	0.02	<0.02	<0.02	<0.02	<0.02	<0.02	0.07	0.06	0.06	0.06	0.06	0.06
Al <sub>2</sub> O <sub>3</sub>	11.46	11.64	14.54	14.67	13.86	14.54	14.51	13.90	13.99	14.67	14.54	14.37	14.72	14.09
Fe <sub>2</sub> O <sub>3</sub>	0.61	0.28	1.26	1.03	0.51	0.81	0.88	1.02	0.94	0.55	0.16	0.40	1.45	1.24
FeO	1.58	1.89	1.87	1.42	1.73	1.25	1.74	2.62	0.76	1.44	1.56	1.41	0.81	1.12
MnO	0.05	0.05	0.04	0.02	0.03	0.02	0.02	0.05	0.01	0.01	0.01	0.01	0.01	0.01
MgO	0.64	0.84	0.28	0.22	0.25	0.28	0.21	0.46	0.27	0.39	0.27	0.26	0.28	0.39
CaO	1.54	1.45	<0.02	<0.02	0.15	0.16	<0.02	0.08	0.09	0.32	0.29	0.19	0.11	0.20
Na <sub>2</sub> O	2.25	1.87	0.35	0.47	2.53	1.84	2.05	0.48	0.12	1.04	2.02	2.30	0.15	0.12
K <sub>2</sub> O	4.33	4.07	6.90	6.25	4.46	4.09	5.19	4.31	4.08	5.53	5.71	5.05	4.20	4.22
P <sub>2</sub> O <sub>5</sub>	<0.03	<0.03	0.04	0.07	0.04	0.04	0.04	0.03	0.06	0.04	0.04	0.04	0.22	0.27
LOI	0.58	0.64	1.51	1.52	1.08	1.36	0.99	1.79	1.87	1.46	1.09	1.07	1.90	1.79
H <sub>2</sub> O <sup>-</sup>	0.02	<0.01	0.17	0.21	0.28	0.18	0.21	0.11	0.06	0.03	0.04	0.03	0.09	0.10
CO <sub>2</sub>	<0.06	0.11	<0.06	<0.06	<0.06	<0.06	0.07	<0.06	<0.06	<0.06	<0.06	<0.06	<0.06	0.13
Total	100.06	99.75	99.93	100.32	99.88	99.64	99.79	100.03	99.60	99.70	99.61	99.88	99.56	99.56
Rb, ppm	125	136	155	201	126	153	144	132	139	154	143	123	133	137
Sr	54	52	31	40	43	37	31	9	17	72	61	45	17	20
Y	85	101	6	5	6	6	5	5	5	6	6	6	4	5
Zr	265	239	81	82	79	80	77	72	74	77	74	69	74	77
Nb	28	24	10	11	11	10	10	10	10	10	10	9	10	10
Ba	653	662	1338	1469	876	655	740	435	305	851	1344	933	376	354
La	48.87	56.65	7.41	9.10	16.74	18.90	13.71	14.70	4.09	12.73	17.01	14.30	10.44	10.76
Ce	110.23	116.13	13.98	21.17	38.33	34.89	35.00	30.63	9.35	26.90	36.08	28.88	23.64	22.36
Pr	12.41	14.86	1.66	2.75	3.95	3.91	3.43	3.81	1.18	3.16	4.33	3.56	2.92	2.60
Nd	48.80	59.43	6.10	9.98	14.43	14.23	13.07	14.07	4.47	11.65	16.18	13.26	10.10	9.32
Sm	11.62	13.82	1.46	2.39	2.95	3.30	2.89	3.08	1.21	2.52	3.16	3.10	2.02	2.05
Eu	1.23	1.43	0.43	0.41	0.53	0.72	0.82	0.84	0.35	0.49	0.51	0.52	0.42	0.45
Gd	8.81	11.31	1.12	1.30	1.80	1.92	1.79	1.72	0.99	1.51	1.81	1.72	1.11	1.19
Tb	1.64	2.06	0.17	0.19	0.22	0.24	0.21	0.20	0.14	0.18	0.23	0.22	0.15	0.16
Dy	11.85	14.52	1.12	1.03	1.17	1.27	1.04	0.96	0.84	0.98	1.15	1.11	0.75	0.90
Ho	2.99	3.37	0.24	0.20	0.20	0.23	0.19	0.17	0.17	0.19	0.20	0.19	0.14	0.18
Er	9.17	9.78	0.67	0.49	0.48	0.54	0.43	0.41	0.48	0.49	0.52	0.46	0.36	0.46
Tm	1.51	1.53	0.10	0.07	0.07	0.07	0.06	0.05	0.07	0.08	0.08	0.07	0.05	0.07
Yb	9.49	9.51	0.70	0.47	0.42	0.46	0.39	0.32	0.40	0.45	0.42	0.40	0.33	0.45
Lu	1.60	1.53	0.11	0.07	0.07	0.07	0.06	0.05	0.06	0.07	0.06	0.06	0.05	0.07
Hf	9.60	8.65	2.99	2.91	2.97	2.95	2.79	2.70	2.83	2.84	2.75	2.45	2.71	2.57
Ta	2.32	1.96	0.99	1.16	1.13	1.12	1.41	1.07	1.09	1.04	1.00	1.05	1.05	1.04
Th	20.12	18.83	12.28	13.82	13.37	13.12	12.35	11.91	12.31	12.54	11.86	10.96	12.24	11.91
U	6.06	5.29	4.81	6.71	4.46	4.19	3.45	3.79	6.24	4.38	6.87	3.23	4.85	5.80
f	0.77	0.72	0.91	0.91	0.90	0.88	0.92	0.89	0.86	0.83	0.86	0.87	0.88	0.85
(La/Yb) <sub>n</sub>	3.33	3.86	6.84	12.61	25.60	26.72	22.64	29.52	6.68	18.13	26.34	22.91	20.18	15.53
Eu/Eu*	0.38	0.35	1.03	0.72	0.71	0.89	1.11	1.13	0.99	0.77	0.66	0.70	0.86	0.89
T, °C	837	840	772	779	760	775	761	780	789	768	751	749	789	790

Note.  $f = \text{FeO}^*/(\text{FeO}^* + \text{MgO})$ ,  $\text{FeO}^* = \text{FeO} + 0.8998 \times \text{Fe}_2\text{O}_3$ ;  $\text{Eu}/\text{Eu}^* = \text{Eu}_n/\sqrt{(\text{Sm}_n \times \text{Gd}_n)}$ ;  $n$ , chondrite-normalized values (Wakita et al., 1970);  $T$ , °C, zircon saturation temperature of the melt (Watson and Harrison, 1983).

veinlets may have slightly increased silica content as a result of secondary processes, while alkali contents in felsic volcanic rocks in the Toporok site not necessarily match the original value (certain rocks display anomalously low  $\text{Na}_2\text{O}$  concentrations, while the  $\text{K}_2\text{O}/\text{Na}_2\text{O}$  ratio in volcanic rocks varies from 2 to 35 (Table 3)). Composition points of metadolerites in the Tagul and Toporok sites, as well as metavolcanic rocks with  $\text{SiO}_2$  content of 57.7 wt.% in the  $\text{Al}_2\text{O}_3$ –( $\text{FeO}^* + \text{TiO}_2$ )– $\text{MgO}$  plot (Jensen, 1976), which is better suited for classification of altered rocks compared to TAS plots, are concentrated in the high Fe tholeiitic basalt field; intermediate metavolcanic rocks in the Toporok site fall into the field of andesites and dacites of the tholeiitic series, while felsic metavolcanic rocks in the Toporok site form a continuous sequence from the rhyolite field of the tholeiitic series to the rhyolite field of the calc-alkaline series, and imaging points of felsic volcanic rocks in the Tagul series are located at the interface between rhyolites of the tholeiitic series and dacites of the calc-alkaline series (Fig. 6b). Composition points of metadolerites and metavolcanic rocks with  $\text{SiO}_2$  content of 57.7 wt.% in the  $\text{Zr}/\text{TiO}_2$ – $\text{Nb}/\text{Y}$  plot (Winchester and Floyd, 1977), which is also suitable for the analysis of altered rocks, fall into the andesite/basalt field, intermediate metavolcanic rocks in the Toporok site are located in the andesite field, and felsic volcanic rocks of the Tagul site in the rhyolite field (Fig. 6c). Imaging points of felsic volcanic rocks in the Toporok site were not indicated in the plot, since they display extremely low Y concentrations (4–6 ppm), which makes the use of the plot impossible. Thus, four groups of rocks, which unite rocks with close chemical compositions, may be defined based on the aforementioned classifications as follows: metadolerites of Tagul and Toporok sites and metavolcanic rocks with  $\text{SiO}_2$  content of 57.7 wt.% (mafic igneous rocks); intermediate metavolcanic rocks in the Toporok site; felsic metavolcanic rocks in the Toporok site and felsic metavolcanic rocks in the Tagul site. A geochemical description of the Maltsevka sequence will be given below for each of the four defined groups.

Mafic igneous rocks of the Maltsevka sequence correspond to high Fe tholeiitic basalts and basaltic andesites of the normal-alkaline series by their chemical composition (Fig. 6a–c). The rocks are characterized by moderately high contents of  $\text{TiO}_2 = 1.17$ – $2.25$  wt.% and  $\text{P}_2\text{O}_5 = 0.17$ – $0.25$  wt.%. Geochemical features of the studied mafic rocks are low concentrations of Nb (5–7 ppm), moderate concentrations of La (7–11 ppm) and Th (0.6–1.7 ppm), as well as increased contents of Y (24–48 ppm) and Yb (2.4–4.1 ppm). The mafic rocks under study also display slightly fractionated distribution of rare-earth elements ( $(\text{La}/\text{Yb})_n = 1.3$ – $2.3$ ) (Fig. 7a). Multielement plots normalized for primitive mantle (Sun and McDonough, 1989) show different spectra in the domain of strongly incompatible elements and close or parallel spectra in the domain of moderately or slightly incompatible elements, along with weakly expressed negative Nb–Ta anomaly, pronounced negative Sr anomaly, and weakly expressed positive Ti anomalies (Fig. 7b).

Intermediate metavolcanic rocks in the Toporok site in terms of their chemical composition are the most similar to normal-alkaline andesites of the tholeiitic series (Fig. 6a–c). The rocks display moderately high Mg# values of 39–46 (Table 2). Intermediate metavolcanic rocks have lower  $\text{TiO}_2$  and Sr contents and higher Ba, Nb, LREE, Th, and U contents compared to mafic rocks (Table 2). Concentrations of elements, such as Y, Zr, and HREE are similar in intermediate and mafic rocks (Table 2). Fractionated distribution of rare-earth elements with  $(\text{La}/\text{Yb})_n = 8$ – $10$  is common for meta-andesites, while negative tilts of the spectra are observed in the domain of light rare-earth elements ( $(\text{La}/\text{Sm})_n = 3$ – $6$ ) and flat spectra in the domains of medium and heavy rare-earth elements ( $(\text{Gd}/\text{Yb})_n = 1$ – $1.5$ ), along with weakly expressed or absent negative europium anomaly ( $\text{Eu}/\text{Eu}^* = 0.56$ – $1.01$ ) (Fig. 7c). Multielement spectra for andesites reveal the mismatch in the domain of strongly incompatible elements (Rb, Ba, and K), while the spectra are similar or parallel in domains of other elements with negative (Nb–Ta, Sr, and Ti) and positive anomalies (Th–U) (Fig. 7d).

Felsic metavolcanic rocks in the Toporok site correspond to rhyolites of the normal-alkaline series in terms of their geochemical features (Fig. 6a–c). The rocks belong to the tholeiitic series and display high iron index ( $f = 0.83$ – $0.92$ ) (Table 3). Metarhyolites show high  $\text{Al}_2\text{O}_3$  contents of 13.9–14.7 wt.%, low  $\text{TiO}_2$  contents below 0.07 wt.%, as well as varying  $\text{Na}_2\text{O}$  concentrations of 0.12–2.53 and increased  $\text{K}_2\text{O}$  concentrations of 4.1–6.9 wt.% (Table 3). Contents of the latter two elements may be altered rather significantly as a result of secondary rock alterations, and contents of large-ion lithophile elements may thus not match with the original values as well. Specific features of felsic volcanic rocks in the Toporok site include low contents of Y (4–6 ppm), Nb (9–11 ppm), Zr (69–82 ppm), La (4–19 ppm), and increased Th concentrations (11–14 ppm) (Table 3). The rocks show strongly fractionated spectra of rare-earth elements ( $(\text{La}/\text{Yb})_n = 7$ – $30$ ) with absence of the europium anomaly ( $\text{Eu}/\text{Eu}^* = 0.66$ – $1.13$ ) (Fig. 7e). Negative Nb, Sr, and Ti anomalies and positive Th–U anomalies are observed in multielement spectra (Fig. 7f). Despite high iron index, felsic metavolcanic rocks in the Toporok site are similar to I-type granites in terms of rare-earth element contents (Chappell and White, 1992).

Felsic metavolcanic rocks in the Tagul site are different from felsic metavolcanic rocks in the Toporok site in terms of their geochemical features, even though they are also typified as rhyolites of the normal-alkaline series (Fig. 6a–c). Metarhyolites in the Tagul site have low iron index ( $f = 0.72$ – $0.77$ ), moderately high contents of  $\text{MgO} = 0.64$ – $0.84$  wt.% and  $\text{CaO} = 1.45$ – $1.54$  wt.% for rhyolites and low concentrations of  $\text{TiO}_2 = 0.14$ – $0.18$  wt.%,  $\text{Al}_2\text{O}_3 = 11.46$ – $11.64$  wt.%, and  $\text{P}_2\text{O}_5 < 0.03$  wt.% (Table 3). High contents of Zr (239–265 ppm), Y (85–100 ppm), Nb (24–28 ppm), La (49–57 ppm), and Th (19–20 ppm) are typical for metavolcanic rocks (Table 3). Metarhyolites in the Tagul site show moderately fractionated spectra of rare-earth elements ( $(\text{La}/\text{Yb})_n = 3$ – $4$ ) and pronounced negative europium anomaly

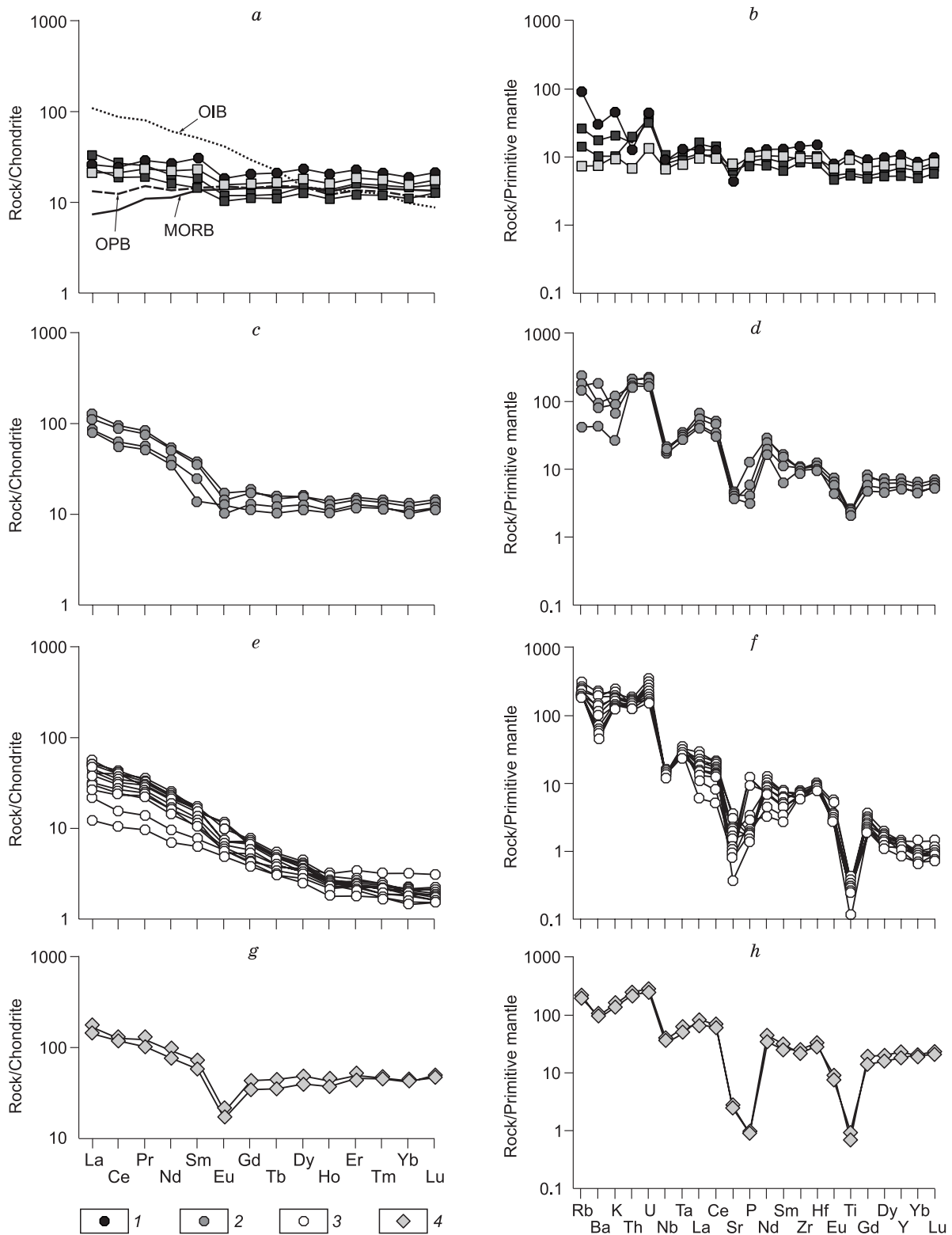


**Fig. 7.** Distribution of trace and rare-earth elements in igneous rocks of the Maltseva sequence of the Elash Group. Chondrite-normalized (Wakita et al., 1970) (a, c, e, g) and primitive mantle normalized contents of elements (Sun and McDonough, 1989) (b, d, f, h). 1, basaltic meta-andesites of the Toporok site; 2, meta-andesites of the Toporok site; 3, metazhyolites of the Toporok site; 4, metazhyolites of the Tagul site. Other designations see Fig. 6. OIB and MORB spectra are shown according to (Sun and McDonough, 1989), and OPB (oceanic plateau basalts) according to (Mahoney et al., 1993).

(Eu/Eu\* = 0.35–0.38) (Fig. 7g). Parallel spectra with negative Nb–Ta, Sr, P, and Ti anomalies are observed in multi-element spectra for metavolcanic rocks (Fig. 7h). Metarhyolites in the Tagul site may be typified as both *I*-type and *A*-type granites based on contents of petrogenic elements (Chappell and White, 1992; Whalen et al., 1987). At the same time, concentrations of trace and rare-earth elements in them imply that they are close to *A*-type granites (Whalen et al., 1987).

## Nd ISOTOPE GEOCHEMISTRY

The data on Nd isotope composition indicates that rocks with both positive and negative  $\epsilon_{\text{Nd}}(T)$  values are present in the Maltsevka sequence (Table 4). Metamorphosed dolerites of Toporok and Tagul sites have close positive  $\epsilon_{\text{Nd}}(T)$  values of +3.7 and +4.1, respectively (Table 4, Fig. 8). Positive  $\epsilon_{\text{Nd}}(T)$  value of +2.2 was also calculated for metarhyolites in the Tagul site. Nd model isotopic age for this rock is 2.2 Ga. At the same time, meta-andesite in the Toporok site displays negative  $\epsilon_{\text{Nd}}(T)$  value of –4.6 with late Archean Nd model isotopic age ( $T(\text{DM}) = 2.6$  Ga) (Table 4, Fig. 8). Negative  $\epsilon_{\text{Nd}}(T)$  value of –3.7 and  $T(\text{DM}) = 2.7$  Ga were calculated for metarhyolites in the Toporok site as well (Table 4, Fig. 8).

## DISCUSSION

### *Petrogenesis of magmatic rocks of the Maltsevka sequence*

Mafic igneous rocks of the Maltsevka sequence (metadolerites and metavolcanic rocks) are close to intraplate basalts in terms of their compositions (Gladkochub et al., 2001; Turkina, 2014). The rocks display reduced magnesium index ( $\text{Mg}\# = 45\text{--}48$ ), moderately high concentrations of  $\text{TiO}_2$  (1.17–2.25 wt.%) and  $\text{P}_2\text{O}_5$  (0.17–0.25 wt.%) (Table 2), and rare-earth element concentrations 10 times as high as those in chondrites (Fig. 7a). Trace element contents and distribution plots of rare-earth and trace elements for metadolerites and metabasaltoids are similar to the plots for oceanic plateau basalts with flat spectra of rare-earth ele-

ments, while different from the plots for classical OIB-type basalts (Fig. 7a, b). Despite the significant secondary alterations, mafic rocks show rather good correlations between La and Nb ( $r = 0.89$ ), La and Th ( $r = 0.81$ ) with lack of correlation between these pairs and losses on ignition (LOI), which makes it possible La, Nb, and Th for classification of rock sources. The rocks analyzed display weakly expressed negative Nb anomaly in multi-element spectra ( $\text{Nb}/\text{Nb}^* = 0.51\text{--}0.80$ ,  $(\text{Nb}/\text{La})_{\text{PM}} = 0.56\text{--}0.70$ ), however,  $(\text{Th}/\text{La})_{\text{PM}}$  and  $(\text{La}/\text{Sm})_n$  indicator ratio values both under and over 1 are common for them (Table 2). These ratios of elements in total with positive  $\epsilon_{\text{Nd}}(T)$  values calculated for metamorphosed dolerites in Toporok and Tagul sites may indicate that an insignificant negative Nb anomaly in multi-element spectra may be the characteristic of their mantle sources, rather than the result of crustal contamination (Kerrick et al., 1999; Turkina and Nozhkin, 2008). Composition points of igneous rocks of the Maltsevka Formation in Nb/Y–Zr/Y (Condie, 2005) and Ce/Nb–Th/Nb (Saunders et al., 1988) plots fall into domains of oceanic plateau basalts (Fig. 9a, b). Since the Paleoproterozoic rocks of the Elash Group, which includes the Maltsevka sequence, were formed within the Elash graben overlaying late Archean rocks, the oceanic plateau is not considered the geodynamic formation setting for dolerites and basaltoids of the Maltsevka sequence. The case under consideration makes it possible to discuss the composition of the mantle subjected to melting under the continental Biryusa block, which is close to oceanic plateau basalts in terms of geochemical isotope parameters. The mixing of the depleted asthenospheric mantle and plume mantle in the source area with no significant effect of the lithospheric mantle appears to be the most likely scenario.

Intermediate metavolcanic rocks as compared to mafic rocks are characterized by increased contents of elements prevailing in the continental crust, i.e., La, Th, and U. Geochemical indicator ratios comparable to those in the continental crust ( $(\text{La}/\text{Sm})_n = 3.2\text{--}6.0$ ,  $(\text{Th}/\text{La})_{\text{PM}} = 3.3\text{--}4.4$ , and  $(\text{Nb}/\text{La})_{\text{PM}} = 0.32\text{--}0.43$ ), along with multi-element spectra with pronounced negative Nb and Ti anomalies and negative  $\epsilon_{\text{Nd}}(T)$  values are typical for meta-andesites (Tables 2 and 4, Fig. 7c, d). At the same time, meta-andesites have moderately high  $\text{Mg}\#$  values (39–46) slightly lower or matching

**Table 4.** Sm–Nd isotopic data results for igneous rocks of the Maltsevka sequence of the Elash Group

Sample No.	Rock	Age, Ma	Content, ppm		$^{147}\text{Sm}/^{144}\text{Nd}$	$^{143}\text{Nd}/^{144}\text{Nd}$ $\pm 2\sigma$	$\epsilon_{\text{Nd}}(T)$	$T_{\text{Nd}}(\text{DM})$ , Ma	$T_{\text{Nd}}(\text{DM-2st})$ , Ma
			Sm	Nd					
Tagul site									
1528	Metadolerite	1870	3.7	10.7	0.1854	$0.512706 \pm 16$	4.1	–	2028
1527	Metarhyolite	1870	7.5	31.0	0.1301	$0.511930 \pm 14$	2.2	2220	2182
Toporok site									
1514	Metadolerite	1870	2.7	8.8	0.1636	$0.512417 \pm 7$	3.7	–	2061
1512	Meta-andesite	1870	5.7	28.7	0.1082	$0.511312 \pm 10$	–4.6	2645	2742
1520	Metarhyolite	1870	2.8	12.1	0.1269	$0.511592 \pm 13$	–3.7	2725	2662

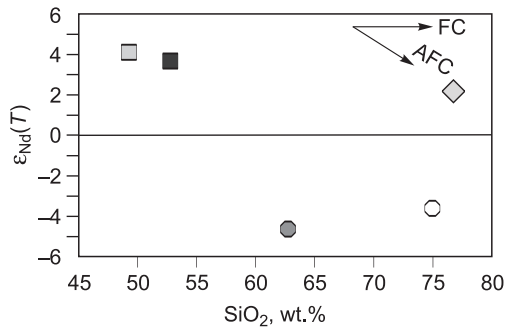


**Fig. 8.**  $\epsilon_{Nd}(T)$ ,  $SiO_2$  plot for igneous rocks of the Maltsevka sequence of the Elash Group. See Figs. 6, 7 for designations. FC, fractional crystallization trend, AFC, simultaneous assimilation and fractional crystallization.

those of mafic rocks of the Maltsevka sequence. The data available make it possible to assume that andesites were formed as a result of crustal source melting with possible participation of the mantle material. In theory, andesites could also be derived from mafic magmas formed by the lithospheric mantle and characterized by negative  $\epsilon_{Nd}(T)$  values. However, mafic metavolcanic rocks of the Maltsevka sequence turned out to have isotope composition and contents of main petrogenic oxides and trace elements comparable to those of similarly aged tonalites of the Podporog massif and diorites of the Uda massif of the Biryusa uplift (Fig. 10a–c), whose formation was associated with the melting of the late Archean diorite-tonalite-gneiss crustal source with addition of juvenile mantle material (Turkina et al., 2006). Thus, andesites of the Maltsevka sequence were most likely formed as a result of melting of a mixed mantle-crustal source.

Felsic metavolcanic rocks in the Tagul site are characterized by rare-earth element compositions close to those of *A*-type granites with high concentrations of Zr, Y, Nb, Th, and REE (aside from Eu). At the same time, the rocks display low  $FeO^*/(FeO^* + MgO)$  ratio values of 0.72–0.77, which in total with low  $Al_2O_3$  concentrations (11.5–11.6 wt.%) makes it possible to only compare metarhyolites in the Tagul site to the oxidized *A*-type granites or even calc-alkaline granites (Dall’Agnol and Oliveira, 2007). Zircon saturation temperatures of the melt were estimated using zircon thermometer developed by E.B. Watson and T.M. Harrison (Watson and Harrison, 1983) at  $\sim 840$  °C (Table 3), i.e., they are moderately high for melts with *A*-type granite properties (Creaser and White, 1991; Skjerlie and Johnston, 1993; King et al., 1997). Thus, it may be assumed that initial rhyolitic melts in the Tagul site were formed in oxidizing conditions under increased  $H_2O$  activity. Metarhyolites analyzed in the Tagul site have positive  $\epsilon_{Nd}(T)$  value of +2.2, which is only slightly less radiogenic, than that of metadolerites of the Maltsevka sequence (Fig. 8). In addition, metarhyolites and mafic igneous rocks show partially overlapping high Y/Nb values (3.02–4.20 in metarhyolites and 4.2–7.9 in mafic igneous rocks) acting as indicators for assessment of source compositions of *A*-type acid igneous rocks (Eby, 1992).

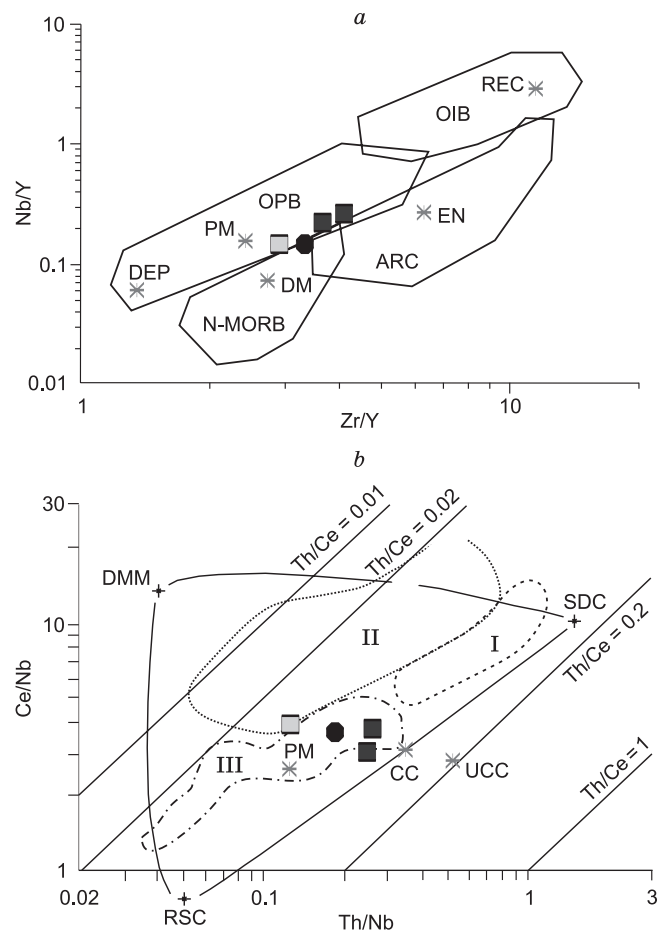


**Fig. 9.** Nb/Y–Zr/Y (Condie, 2005) (a) and Ce/Nb–Th/Nb (Saunders et al., 1988) (b) plots for mafic igneous rocks of the Maltsevka sequence of the Elash Group. See Fig. 6 for designations. Domains in the plot (b) according to (Turkina and Nozhkin, 2008) are as follows: I, island-arc basalts; II, Lau back-arc basin basalts; III, Ontong Java and Broken Ridge oceanic plateau basalts. ARC, island-arc basalts; N-MORB, mid-ocean ridge basalts; OIB, oceanic island basalts; OPB, oceanic plateau basalts; DM, depleted mantle; PM, primitive mantle; DEP, deep depleted mantle; REC, recycled mantle; EN, enriched mantle; DMM, depleted MORB mantle; RSC, oceanic crustal restite; SDC, subduction mantle; CC, continental crust; UCC, upper continental crust.

Thus, *A*-type rhyolite formation in the Tagul site was most likely associated with the melting of the source close to basic igneous rocks of the Maltsevka sequence in terms of isotope parameters. As of now, no rocks with isotope and chemical compositions completely similar to those of rhyolites of the Tagul site are observed among granitoids of the Sayan complex (Fig. 10).

Despite the high iron index, felsic metavolcanic rocks in the Toporok site show increased  $Al_2O_3$  concentrations of 13.9–14.7 wt.% with  $SiO_2$  contents of 73–77 wt.%, low contents of Y, Nb, Zr, and La, and fractionated spectra of rare-earth elements ( $(La/Yb)_n = 7–30$ ), which makes it possible to compare them to *I*-type granites. Zircon saturation temperatures of the melt for metarhyolites of the Toporok site are 750–790 °C (Table 3), which corresponds to temperatu-

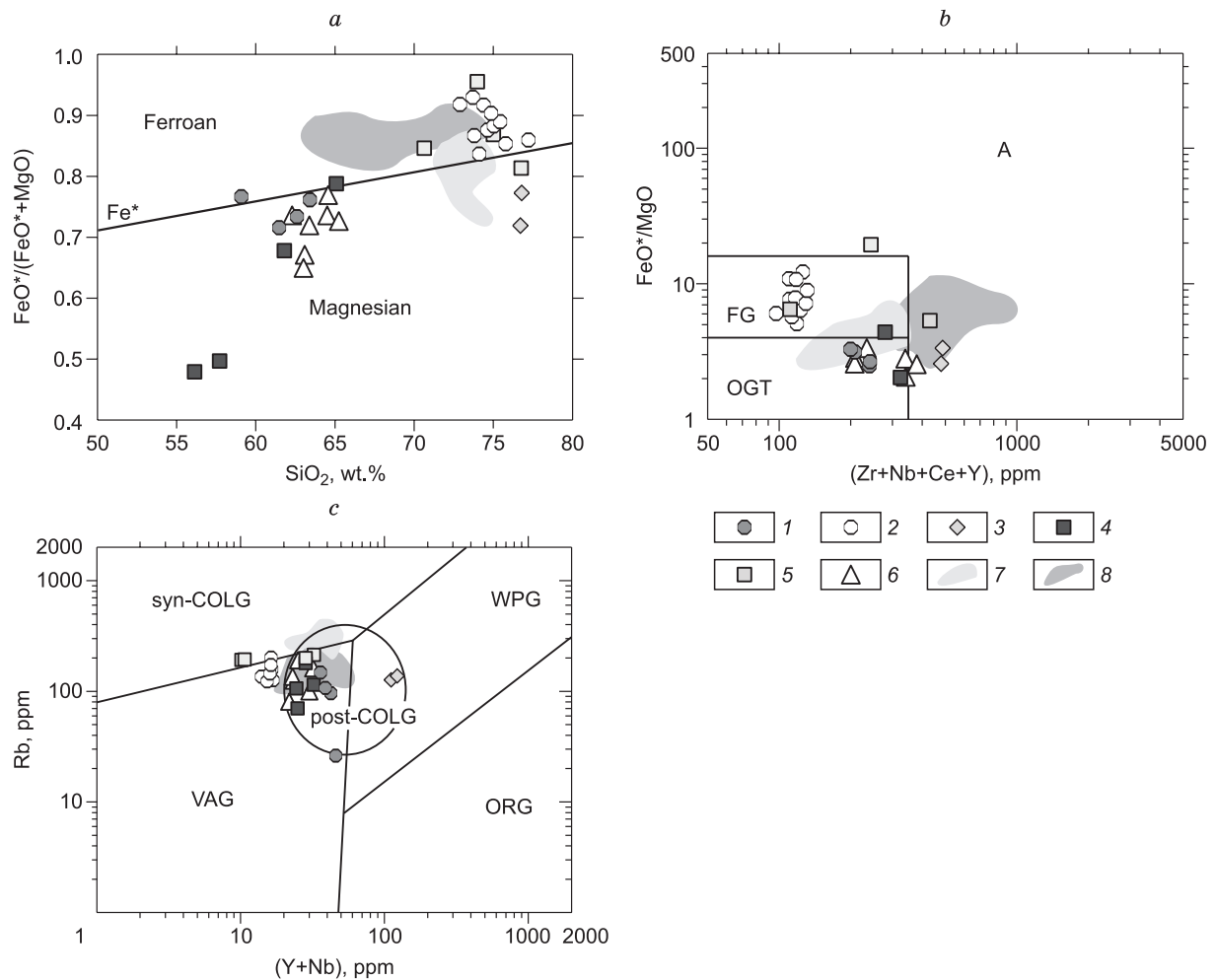


**Fig. 10.**  $\text{FeO}^*/(\text{FeO}^* + \text{MgO})$ – $\text{SiO}_2$  (Frost et al., 2001) (a),  $\text{FeO}^*/\text{MgO}$ – $(\text{Zr} + \text{Nb} + \text{Y} + \text{Ce})$  (Whalen et al., 1987) (b), and  $\text{Rb}$ – $(\text{Y} + \text{Nb})$  (Pearce, 1996) (c) plots for igneous rocks of the Sayan–Biryusa volcanoplutonic belt. 1–3, Maltsevka sequence: 1, meta-andesites of the Toporok site, 2, metarhyolites of the Toporok site, 3, metarhyolites of the Tagul site; 4–8, Sayan complex: 4, diorites of the Uda massif (Turkina et al., 2006), 5, granites and leucogranites of the Uda massif (Turkina et al., 2006), 6, tonalites of the Podporog massif (Turkina et al., 2006), 7, two-mica S-type granite domain of the Biryusa massif (Donskaya et al., 2014), 8, biotite-amphibolic A-type granite domain of the Barbitai massif (Levitskii et al., 2002). Domains in the plot (b): A, A-type granite domain; FG, fractionated *M*-, *I*-, and *S*-type granite domain; OGT, nonfractionated *M*-, *I*-, and *S*-type granite domain. Domains in plot (c): VAG, volcanic arc granites; ORG, oceanic ridge granites; WPG, intraplate granites; syn-COLG, syncollision granites; post-COLG, postcollision granites.

res at initial crystallization stages of high-temperature I-type granites (Chappell et al., 1998). Metarhyolites analyzed in the Toporok site have negative  $\varepsilon_{\text{Nd}}(T)$  values of  $-3.7$ , which makes it possible to consider continental crustal rocks as the source of these metarhyolites. It is believed that crustal metagneous rocks may be the source of I-type felsic rocks in the syncollision setting (Turkina et al., 2006; and references therein). A slightly less radiogenic composition of metarhyolites in the Toporok site compared to late Archean rocks of the Khailama series of the Biryusa block (Turkina et al., 2006), as well as high Th concentrations (11–14 ppm) in metarhyolites indicate that lower crustal diorite-tonalitic rocks may be considered as the most likely source of these metarhyolites with possible addition of juvenile mantle material to the magma generation site. Metarhyolites in the

Toporok site turned out to have similar composition to leucogranites of the Uda massif of the Biryusa uplift (Fig. 10a–c), which are also assumed to have a mixed mantle-crustal source (Turkina et al., 2006).

Thus, the data obtained make it possible to conclude that Maltsevka sequence of the Elash Group unites volcanic rocks of similar ages with various compositions. Originally the magmatism could have been caused by movement of the mantle material towards the crustal base followed by its intrusions in the form of doleritic and mafic volcanic dikes. In addition, mantle melts acted as the heat source that caused continental crustal melting in the Biryusa block, as well as the source of mantle material in process of formation of mixed mantle-crustal parental melts for intermediate and felsic rocks in the Toporok site.

## Tectonic consequences

U–Pb isotopic age estimates for metarhyolites of the Maltsevka sequence in the Tagul and Toporok sites turned out to be almost identical ( $1872 \pm 10$  and  $1874 \pm 10$  Ma, respectively) and overlapping within the measurement error with age estimates for granitoids of the Sayan complex of the Biryusa block (1.90–1.86 Ga) (Levitskii et al., 2002; Turkina et al., 2003, 2006; Donskaya et al., 2014; Makagon et al., 2015). Thus, volcanic rocks of the Elash Group and granitoids of the Sayan complex may be united into a single volcanoplutonic association based on closeness of their ages and geological positions. In addition, the aforementioned similarity of isotope and chemical compositions between intermediate and felsic metavolcanic rocks in the Toporok site of the Maltsevka sequence and granitoids of the Uda massif of the Sayan complex (Fig. 10) is also an argument in favor of identification of a single volcanoplutonic association.

It was repeatedly noted earlier (Turkina et al., 2006; Galimova et al., 2012; Donskaya et al., 2014) that Paleoproterozoic granitoids in the Biryusa block form a single extensive magmatic belt. The results of geochronological and geochemical isotope studies of igneous rocks of the Maltsevka sequence of the Elash Group presented in this paper made it possible to extend this belt via combining granitoids and volcanic rocks into a single volcanoplutonic association and thereby identify a volcanoplutonic rather than granitoid belt. The belt referred to as Sayan–Biryusa belt stretches over about 300 km in the NW direction along the junction zone between the Biryusa block of the Angara fold belt and Archean Tunguska superterrane of the Siberian craton (Figs. 1, 2). The specific feature of the belt is that it unites granitoids and volcanic rocks of similar ages with heterogeneous geochemical isotope parameters. The presence of *I*-type diorites, tonalites, and rhyolites (Turkina, 2005; Turkina et al., 2006; the present paper), two-mica *S*-type granites (Donskaya et al., 2014), *A*-type granites and rhyolites (Levitskii et al., 2002; Turkina et al., 2006; the present paper), and basic igneous rocks is observed in the Sayan–Biryusa belt. It was shown earlier in (Donskaya et al., 2014) that postcollisional granitoids of the Biryusa block were formed at increased temperatures within the syncollisional structure generated in process of integration of continental blocks and terranes of different geodynamic origins into a single structure, which ensured diversity of substrates subjected to melting and thus led to the formation of granitoids with various compositions. It was assumed in the cited paper that high-temperature values calculated for the granitoids of the Biryusa block are associated with movement of the mantle material towards the crustal basement. The results of isotope studies of magmatic rocks of the Maltsevka sequence of the Elash Group presented in this paper confirm the earlier assumption. It is mafic metadolerites and metavolcanic rocks of the Maltsevka sequence with positive  $\epsilon_{\text{Nd}}(T)$  values that are derivatives of the mantle source at the basement of the Biryusa block. If we apply the discussion of modeling

efforts from (Sylvester, 1998) to the Biryusa block, we may conclude that a major volume of magmatic rocks of close ages with various compositions in the Biryusa block could be associated with lithospheric thinning as a result of delamination that followed the main collision events, which led to uplift of mantle magmas to the crustal basement with their further intrusion into the continental crust, where they could either act as heat sources or interact with the crustal material to form granitoids and volcanic rocks.

The discovery of the Paleoproterozoic volcanoplutonic belt in the Biryusa block made it possible to talk about two Paleoproterozoic belts within the South Siberian postcollisional magmatic belt in the south of the Siberian craton, specifically Sayan–Biryusa and North Baikal volcanoplutonic belts (Fig. 1). Felsic igneous rocks of close ages with similar geological positions, i.e., postfolding postmetamorphic structures, prevail in both belts (Neimark et al., 1991, 1998; Levitskii et al., 2002; Larin et al., 2003; Turkina et al., 2003, 2006; Donskaya et al., 2005, 2008, 2014). However, granitoids and felsic volcanic rocks of the Sayan–Biryusa and North Baikal volcanoplutonic belts show significant differences in geochemical parameters. Acid igneous in the North Baikal belt have chemical compositions of *A*-type granites (Neimark et al., 1998; Donskaya et al., 2005, 2008). As for the Sayan–Biryusa belt, it was mentioned earlier that all geochemical types of volcanic rocks and granitoids are encountered there. The following model may be proposed to explain this phenomenon. The South Siberian postcollisional magmatic belt observable in the south of the Siberian craton over a distance of over 2500 km intersects all the main tectonic structures in this part of the craton (Fig. 1) and on the global scale represents a major linking structure that fixed the establishment of the unified Siberian craton (Larin et al., 2003; Gladkochub et al., 2006), as well as its inclusion into the Paleoproterozoic supercontinent Columbia (Didenko et al., 2009). The last collision events in the south of the Siberian craton date back to 1.90–1.87 Ga in the Angara–Kan, Biryusa, and Sharyzhalgai blocks (Aftalion et al., 1991; Poller et al., 2004, 2005; Turkina et al., 2006, 2012; Sal'nikova et al., 2007; Levchenkov et al., 2012; Urmantseva et al., 2012; Nozhkin et al., 2016), 1.92–1.90 Ga in the Aldan shield (Frost et al., 1998; Kotov, 2003; Kotov et al., 2004; Larin et al., 2006), and 1.91–1.88 Ga in the Stanovoi uplift (Larin et al., 2004; Glebovitsky et al., 2008, 2009). These age estimates make it possible to consider the rocks of the South Siberian magmatic belt as postcollision structures. Since Biryusa block was attached to the Siberian craton at about 1.9 Ga (Turkina et al., 2006), i.e., at the final stage of the craton structure formation, the diversity of igneous rock compositions that started forming immediately after collision events in the process of orogenic structure collapse seems inartificial (Sylvester, 1998). The North Baikal volcanoplutonic belt, which may be considered a postcollisional structure on the global scale of formation of the unified structure of the Siberian craton, may also be viewed as an anorogenic structure on the regional scale of the Akitkan

fold belt, which it intersects, since the main collision events within the Akitkan fold belt were finished 1.98–1.97 Ga (Donskaya et al., 2016), i.e., approximately 100 Myr prior to the formation of the rocks of the North Baikal belt. In other words, one might consider that on the local scale the rocks of the North Baikal belt are formed in intraplate settings that favor the formation of the rocks close to A-type granites, which is the case within this volcanoplutonic belt. Thus, the rocks with diverse geochemical parameters, which possibly reflect the specifics of collision events in certain parts of the craton, are unified within the extensive South Siberian Paleoproterozoic postcollisional magmatic belt.

## CONCLUSIONS

U–Pb zircon dating of metarhyolites of the Maltsevka sequence of the Elash Group of the Biryusa block showed ages of  $1872 \pm 10$  and  $1874 \pm 10$  Ma, which match with the age estimates obtained for granitoids of the Sayan complex of the Biryusa block (Levitskii et al., 2002; Turkina et al., 2003, 2006; Donskaya et al., 2014; Makagon et al., 2015). Since volcanic rocks of the Elash Group and granitoids of the Sayan complex of the Biryusa block are similar in terms of age and geological position and are placed within the same structure, they were united a single volcanoplutonic association.

Metamorphosed igneous rocks of the Maltsevka sequence of the Elash Group are represented by volcanic rocks, specifically basaltic andesites, andesites, dacites, and rhyolites, with prevalence of felsic volcanic rocks, and subvolcanic rocks, including dolerites. Based on chemical compositions, the analyzed rocks were divided into four groups: (1) mafic rocks (metadolerites and metavolcanic rocks) close to high Fe tholeiitic basalts and normal-alkaline basaltic andesites in terms of chemical composition; (2) meta-andesites of the normal-alkaline tholeiitic series; (3) normal-alkaline metarhyolites with geochemical parameters of I-type granites; (4) normal-alkaline metarhyolites with geochemical parameters of A-type granites. Overall, the results of geochemical isotope studies make it possible to conclude that the Maltsevka sequence of the Elash Group unites volcanic rocks of similar ages with various compositions.

Mafic igneous rocks of the Maltsevka sequence are close to intraplate basalts in terms of chemical composition. The assumption is that depleted asthenospheric mantle and possibly plume mantle were the sources of these rocks, while lithospheric mantle had no significant effect. Geochemical parameters of meta-andesites imply that they could have been formed as a result of late Archean crustal source melting with participation of the mantle material. Metarhyolites close to A-type granites in terms of trace element composition could have been formed as a result of melting of the source with geochemical isotope parameters close to those of basic igneous rocks of the Maltsevka sequence. Metarhyolites close to I-type granites could have been formed as a result of melting of lower crustal diorite-tonalitic rocks with

possible addition of juvenile mantle material to the magma generation site.

The results of geochronological and geochemical isotope studies made it possible to unite the rocks of the Elash Group and granitoids of the Sayan complex into the Sayan–Biryusa Paleoproterozoic postcollisional volcanoplutonic belt that stretches over a distance of about 300 km along the junction zone between the Biryusa block of the Angara fold belt and the Archean Tunguska superterrane of the Siberian craton. The Sayan–Biryusa belt is a part of a major South Siberian Paleoproterozoic postcollisional magmatic belt generated at the final formation stage of the Siberian craton, when it was possibly a part of Paleoproterozoic supercontinent Columbia.

The authors thank T.A. Kornilova (Institute of the Earth's Crust SB RAS) for the assistance in petrographic studies. The work was supported by the Russian Foundation for Basic Research (project No. 15-05-05863).

## REFERENCES

- Aftalion, M., Bibikova, E.V., Bowes, D.R., Hopgood, A.M., Perchuk, L.L., 1991. Timing of Early Proterozoic collisional and extensional events in the granulite-gneiss-choronite-granite complex, Lake Baikal, USSR: A U–Pb, Rb–Sr, and Sm–Nd isotopic study. *J. Geol.* 99 (6), 851–861.
- Belichenko, V.G., Shmotov, A.P., Sez'ko, A.I., Es'kin, A.E., Vasil'ev, E.P., Reznitskii, L.Z., Boos, R.G., Matison, O.R., 1988. Precambrian and Paleozoic Evolution of the Earth's Crust (Sayan–Baikal Mountain Area) [in Russian]. Nauka, Novosibirsk.
- Black, L.P., Kamo, S.L., Allen, C.M., Aleinikoff, J.N., Davis, D.W., Korsch, R.J., Foudoulis, C., 2003. TEMORA 1: a new zircon standard for Phanerozoic U–Pb geochronology. *Chem. Geol.* 200 (1–2), 155–170.
- Chappell, B.W., White, A.J.R., 1992. I- and S-type granites in the Lachlan Fold Belt, in: *Earth Environ. Sci. Trans. R. Soc. Edinburgh*, Vol. 83 (Second Hutton Symposium: The Origin of Granites and Related Rocks), pp. 1–26.
- Chappell, B.W., Bryant, C.J., Wyborn, D., White, A.J.R., Williams, I.S., 1998. High- and low-temperature I-type granites. *Res. Geol.* 48 (4), 225–235.
- Condie, K.C., 2005. High field strength element ratios in Archean basalts: a window to evolving sources of mantle plumes? *Lithos* 79 (3–4), 491–504.
- Creaser, R.A., White, A.J.R., 1991. Yardea dacite—large-volume, high-temperature felsic volcanism from the Middle Proterozoic of South Australia. *Geology* 19 (1), 48–51.
- Dall'Agnol, R., Oliveira, D.C., 2007. Oxidized, magnetite-series, rapakivi-type granites of Carajás, Brazil: Implications for classification and petrogenesis of A-type granites. *Lithos* 93 (3–4), 215–233.
- Didenko, A.N., Vodovozov, V.Y., Pisarevsky, S.A., Gladkochub, D.P., Donskaya, T.V., Mazukabzov, A.M., Stanevich, A.M., Bibikova, E.V., Kirnozova, T.I., 2009. Palaeomagnetism and U–Pb dates of the Palaeoproterozoic Akitkan Group (South Siberia) and implications for pre-Neoproterozoic tectonics, in: *Geol. Soc. London, Spec. Publ.* 323, pp. 145–163.
- Didenko, A.N., Gur'yanov, V.A., Peskov, A.Yu., Perestoronin, A.N., Avdeev, D.V., Bibikova, E.V., Kirnozova, T.I., Fugzan, M.M., 2010. Geochemistry and geochronology of the Proterozoic igneous rocks of the Ulkan trough: New data. *Russ. J. Pacific Geol.* 4 (5), 398–417.
- Dmitrieva, N.V., Nozhkin, A.D., 2012. Geochemistry of the Paleoproterozoic metaterrigenous rocks of the Biryusa Block, southwestern Siberian Craton. *Lithol. Min. Resour.* 47 (2), 138–159.

- Donskaya, T.V., Gladkochub, D.P., Kovach, V.P., Mazukabzov, A.M., 2005. Petrogenesis of early Proterozoic postcollisional granitoids in the southern Siberian craton. *Petrology* 13 (3), 229–252.
- Donskaya, T.V., Bibikova, E.V., Gladkochub, D.P., Mazukabzov, A.M., Bayanova, T.B., De Waele, B., Didenko, A.N., Bukharov, A.A., Kimozova, T.I., 2008. Petrogenesis and age of the felsic volcanic rocks from the North Baikal volcanoplutonic belt, Siberian craton. *Petrology* 16: 422. DOI:10.1134/S0869591108050020.
- Donskaya, T.V., Gladkochub, D.P., Mazukabzov, A.M., Wingate, M.T.D., 2014. Early Proterozoic postcollisional granitoids of the Biryusa block of the Siberian craton. *Russian Geology and Geophysics (Geologiya i Geofizika)* 55 (7), 812–823 (1028–1043).
- Donskaya, T.V., Gladkochub, D.P., Mazukabzov, A.M., Lepekhnina, E.N., 2016. Age and sources of the Paleoproterozoic premetamorphic granitoids of the Goloustnaya block of the Siberian craton: geodynamic applications. *Petrology* 24 (6), 543–561.
- Eby, G.N., 1992. Chemical subdivision of the A-type granitoids: Petrogenetic and tectonic implications. *Geology* 20 (7), 641–644.
- Frost, B.R., Avchenko, O.V., Chamberlain, K.R., Frost, C.D., 1998. Evidence for extensive Proterozoic remobilization of the Aldan shield and implications for Proterozoic plate tectonic reconstructions of Siberia and Laurentia. *Precambrian Res.* 89 (1–2), 1–23.
- Frost, B.R., Barnes, C.G., Collins, W.J., Arculus, R.J., Ellis, D.J., Frost, C.D., 2001. A geochemical classification for granitic rocks. *J. Petrology* 42 (11), 2033–2048.
- Galimova, T.F., Pashkova, A.G., Povarintseva, S.A., Perfil'ev, V.V., Namolova, M.M., Andryushchenko, S.V., Denisenko, E.P., Permyakov, S.A., Mironyuk, E.P., Timashkov, A.N., Plekhanov, A.O., 2012. National Geological Map of the Russian Federation. Scale 1:1,000,000, third generation. Angara–Yenisei Series. Sheet N-47—Nizhneudinsk. Explanatory Note [in Russian]. VSEGEI, St. Petersburg.
- Gladkochub, D.P., Sklyarov, E.V., Donskaya, T.V., Mazukabzov, A.M., Men'shagin, Yu.V., Panteeva, S.V., 2001. Petrology of gabbro-dolerites from Neoproterozoic dike swarms in the Sharyzhalgai block with reference to the problem of breakup of the Rodinia supercontinent. *Petrology* 9 (6), 560–575.
- Gladkochub, D., Pisarevsky, S.A., Donskaya, T., Natapov, L.M., Mazukabzov, A., Stanevich, A.M., Silkyarov, E., 2006. The Siberian Craton and its evolution in terms of Rodinia hypothesis. *Episodes* 29 (3), 169–174.
- Glebovitsky, V.A., Sedova, I.S., Berezhnaya, N.G., Presnyakov, S.I., Samorukova, L.M., 2008. Age of migmatites in the Stanovoi Complex, east Siberia: Results of zircon dating by the SHRIMP-II U–Pb method. *Dokl. Earth Sci.* 420 (1), 542–546.
- Glebovitsky, V.A., Kotov, A.B., Sal'nikova, E.B., Larin, A.M., Velikoslavinsky, S.D., 2009. Granulite complexes of the Dzhugdzhur–Stanovoi Fold Region and Peristanovoi belt: Age, formation conditions, and geodynamic settings of metamorphism. *Geotectonics* 43 (4), 253–263.
- Goldstein, S.J., Jacobsen, S.B., 1988. Nd and Sr isotopic systematics of rivers water suspended material: implications for crustal evolution. *Earth Planet. Sci. Lett.* 87 (3), 249–265.
- Jacobsen, S.B., Wasserburg, G.J., 1984. Sm–Nd isotopic evolution of chondrites and achondrites, II. *Earth Planet. Sci. Lett.* 67 (2), 137–150.
- Jensen, L.S., 1976. A New Cation Plot for Classifying Subalkalic Volcanic Rocks. Miscellaneous, Ontario Department of Mines.
- Kerrick, R., Polat, A., Wyman, D., Hollings, P., 1999. Trace element systematics of Mg-, to Fe-tholeiitic basalt suites of the Superior Province: implications for Archean mantle reservoirs and greenstone belt genesis. *Lithos* 46 (1), 163–187.
- King, P.L., White, A.J.R., Chappell, B.W., Allen, C.M., 1997. Characterization and origin of aluminous A-type granites from the Lachlan fold belt, Southeastern Australia. *J. Petrol.* 38 (3), 371–391.
- Kotov, A.B., 2003. Boundary Conditions for Geodynamic Models of Continental Crust Formation in the Aldan Shield. ScD Thesis [in Russian]. SPGU, St. Petersburg.
- Kotov, A.B., Sal'nikova, E.B., Larin, A.M., Kovach, V.P., Savatenkov, V.M., Yakovleva, S.Z., Berezhnaya, N.G., Plotkina, Yu.V., 2004. Early Proterozoic granitoids in the junction zone of the Olekma granite-greenstone belt and the Aldan granulite-gneiss terrane, Aldan Shield: age, sources, and geodynamic environments. *Petrology* 12 (1), 37–55.
- Larin, A.M., 2011. Rapakivi Granites and Associating Rocks [in Russian]. Nauka, St. Petersburg.
- Larin, A.M., 2014. Ulkan-Dzhugdzhur ore-bearing anorthosite-rapakivi granite-peralkaline granite association, Siberian Craton: Age, tectonic setting, sources, and metallogeny. *Geol. Ore Deposits* 56 (4), 257–280.
- Larin, A.M., Amelin, Yu.V., Neymark, L.A., Krimsky, R.Sh., 1997. The origin of the 1.73–1.70 Ga anorogenic Ulkan volcanoplutonic complex, Siberian Platform, Russia: inferences from geochronological, geochemical and Nd–Sr–Pb isotopic data. *Anais da Academia Brasileira de Ciencias* 69 (3), 295–312.
- Larin, A.M., Sal'nikova, E.B., Kotov, A.B., Kovalenko, V.I., Ryt'sk, E.Yu., Yakovleva, S.Z., Berezhnaya, N.G., Kovach, V.P., Buldygerov, V.V., Sryvtsev, N.A., 2003. The North Baikal volcanoplutonic belt: age, formation duration, and tectonic setting. *Dokl. Earth Sci.* 392 (7), 963–967.
- Larin, A.M., Sal'nikova, E.B., Kotov, A.B., Glebovitsky, V.A., Kovach, V.P., Berezhnaya, N.G., Yakovleva, S.Z., Tolkachev, M.D., 2004. Late Archean granitoids of the Dambukinskii block of the Dzhugdzhur–Stanovoy fold belt: formation and transformation of the continental crust in the early Precambrian. *Petrology* 12 (3), 211–226.
- Larin, A.M., Sal'nikova, E.B., Kotov, A.B., Makar'ev, L.B., Yakovleva, S.Z., Kovach, V.P., 2006. Early Proterozoic syn- and postcollision granites in the northern part of the Baikal fold area. *Stratigr. Geol. Corr.* 14 (5), 463–474.
- Larin, A.M., Kotov, A.B., Velikoslavinskii, S.D., Sal'nikova, E.B., Kovach, V.P., 2012. Early Precambrian A-granitoids in the Aldan Shield and adjacent mobile belts: sources and geodynamic environments. *Petrology* 20 (3), 218–239.
- Levchenkov, O.A., Levitskii, V.I., Rizvanova, N.G., Kovach, V.P., Sergeeva, N.A., Levskii, L.K., 2012. Age of the Irkut block of the Prisanay uplift of the Siberian Platform basement: dating minerals from metamorphic blocks. *Petrology* 20 (1), 86–92.
- Levitskii, V.I., Mel'nikov, A.I., Reznitskii, L.Z., Bibikova, E.V., Kirnozova, T.I., Kozakov, I.K., Makarov, V.A., Plotkina, Yu.V., 2002. Early Proterozoic postcollisional granitoids in southwestern Siberian craton. *Geologiya i Geofizika (Russian Geology and Geophysics)* 43 (8), 717–731 (679–692).
- Ludwig, K.R., 1999. User's Manual for Isoplot/Ex, Version 2.10, A Geochronological Toolkit for Microsoft Excel. Berkeley: Berkeley Geochronology Center, Spec. Publ. 1a.
- Ludwig, K.R., 2000. SQUID 1.00: A User's manual. Berkeley: Berkeley Geochronology Center, Spec. Publ. 2.
- Mahoney, J.J., Storey, M., Duncan, R.A., Spencer, K.J., Pringle, M., 1993. Geochemistry and age of the Ontong Java Plateau, in: *The Mesozoic Pacific: Geology, Tectonics, and Volcanism*. AGU, Washington, D.C.: Geophys. Monogr. Ser., Vol. 77, pp. 233–261.
- Makagon, V.M., Bayanova, T.B., Zagorskii, V.E., 2015. Synchronous early Precambrian I- and A-type granite massifs in rare metallic pegmatite fields of the East-Sayan belt, in: *Proc. Meet. "Geodynamic Evolution of the Lithosphere of the Central Asian Mobile Belt (Ocean to Continent)"*, Vol. 13 [in Russian]. IZK SO RAN, Irkutsk, pp. 144–145.
- Neimark, L.A., Larin, A.M., Yakovleva, S.Z., Sryvtsev, N.A., Buldygerov, V.V., 1991. New data on the age of Akitkan series of the Baikal Patom fold area based on U–Pb zircon dating. *Dokl. Akad. Nauk SSSR* 320 (1), 182–186.
- Neimark, L.A., Larin, A.M., Yakovleva, S.Z., Gorokhovskii, B.M., 1992. U–Pb isotopic age of igneous rocks of the Ulkan graben (southwestern part of the Aldan Shield). *Dokl. Akad. Nauk* 323 (6), 1152–1156.

- Neimark, L.A., Larin, A.M., Nemchin, A.A., Ovchinnikova, G.V., Ryt'sk, E.Yu., 1998. Geochemical, geochronological (U–Pb), and isotopic (Pb, Nd) evidence of anorogenic nature of magmatism in the North-Baikal volcanoplutonic belt. *Petrologiya* 6 (4), 139–164.
- Nozhkin, A.D., Turkina, O.M., Dmitrieva, N.V., Serov, P.A., 2015. Age constraints of Paleoproterozoic metasedimentary complex formation in the southwestern margin of the Siberian craton, in: Proc. 6th Russ. Conf. "Isotopic Geochronology Isotopic Dating of Geological Processes: New Results, Approaches and Prospects" [in Russian]. Springer, St. Petersburg, pp. 194–196.
- Nozhkin, A.D., Turkina, O.M., Likhanov, I.I., Dmitrieva, N.V., 2016. Late Paleoproterozoic volcanic associations in the southwestern Siberian craton (Angara–Kan block). *Russian Geology and Geophysics (Geologiya i Geofizika)* 57 (2), 247–264 (312–332).
- Panteeva, S.V., Gladkochub, D.P., Donskaya, T.V., Markova, V.V., Sandimirova, G.P., 2003. Determination of 24 trace elements in felsic rocks by inductively coupled plasma mass spectrometry after lithium metaborate fusion. *Spectrochim. Acta Part B: Atomic Spectroscopy* 58, 341–350.
- Pearce, J.A., 1996. Sources and settings of granitic rocks. *Episodes* 19 (4), 120–125.
- Pin, C., Zalduogui, J.F.S., 1997. Sequential separation of light rare-earth elements, thorium and uranium by miniaturized extraction chromatography: Application to isotopic analyses of silicate rocks. *Analyt. Chim. Acta* 339 (1–2), 79–89.
- Poller, U., Gladkochub, D.P., Donskaya, T.V., Mazukabzov, A.M., Sklyarov, E.V., Todt, W., 2004. Timing of Early Proterozoic magmatism along the Southern margin of the Siberian Craton (Kitoy area), in: *Earth Environ. Sci. Trans. R. Soc. Edinburgh*, Vol. 95, pp. 215–225.
- Poller, U., Gladkochub, D., Donskaya, T., Mazukabzov, A., Sklyarov, E., Todt, W., 2005. Multistage magmatic and metamorphic evolution in the Southern Siberian Craton: Archean and Paleoproterozoic zircon ages revealed by SHRIMP and TIMS. *Precambrian Res.* 136 (3–4), 353–368.
- Rosen, O.M., 2003. Siberian craton: tectonic zoning and evolutionary stages. *Geotectonika*, No. 3, 3–21.
- Sal'nikova, E.B., Kotov, A.B., Levitskii, V.I., Reznitskii, L.Z., Mel'nikov, V.I., Kozakov, I.K., Kovach, V.P., Barash, I.G., Yakovleva, S.Z., 2007. Age constraints of high-temperature metamorphic events in crystalline complexes of the Irkut block, the Sharyzhalgai ledge of the Siberian platform basement: Results of the U–Pb single zircon dating. *Stratigr. Geol. Corr.* 15 (4), 343–358.
- Saunders, A.D., Norry, M.J., Tarney, J., 1988. Origin of MORB and chemically-depleted mantle reservoirs: trace element constraints. *J. Petrol., Spec. Lithosphere Issue*, 415–445.
- Sharpenok, L.N., Kostin, A.E., Kukharenko, E.A., 2008. Detailed total alkali silica (TAS) diagram for chemical classification of volcanic rocks. *Regional'naya Geologiya i Metallogeniya*, No. 35, 48–55.
- Skjerlie, K.P., Johnston, A.D., 1993. Fluid-absent melting behavior of an F-rich tonalitic gneiss at mid-crustal pressures: implications for the generation of anorogenic granites. *J. Petrol.* 34 (1), 785–815.
- Sun, S.-s., McDonough, W.F., 1989. Chemical and isotopic systematics of oceanic basalts: implications for mantle composition and processes, in: Saunders, A.D., Norry, M.J. (Eds.), *Magmatism in the Ocean Basins*. Geol. Soc. London, Spec. Publ. 42, pp. 313–345.
- Sylvester, P.J., 1998. Post-collisional strongly peraluminous granites. *Lithos* 45 (1–4), 29–44.
- Turkina, O.M., 2005. Proterozoic tonalites and trondhjemites of the southwestern margin of the Siberian craton: isotope geochemical evidence for the lower crustal sources and conditions of melts formation in collisional settings. *Petrology* 13 (1), 35–48.
- Turkina, O.M., 2014. Lectures on Magmatic and Metamorphic Geochemistry [in Russian]. NGU, Novosibirsk.
- Turkina, O.M., Nozhkin, A.D., 2008. Oceanic and riftogenic metavolcanic associations of greenstone belts in the northwestern part of the Sharyzhalgai Uplift, Baikal region. *Petrology* 16 (5), 468–491. DOI:10.1134/S0869591108050044.
- Turkina, O.M., Bibikova, E.V., Nozhkin, A.D., 2003. Stages and geodynamic settings of Early Proterozoic granite formation on the southwestern margin of the Siberian craton. *Dokl. Earth Sci.* 389 (2), 159–163.
- Turkina, O.M., Nozhkin, A.D., Bayanova, T.B., 2006. Sources and formation conditions of Early Proterozoic granitoids from the southwestern margin of the Siberian Craton. *Petrology* 14 (3), 262–283.
- Turkina, O.M., Berezhnaya, N.G., Lepekhina, E.N., Kapitonov, I.N., 2012. U–Pb (SHRIMP II), Lu–Hf isotope and trace element geochemistry of zircons from high-grade metamorphic rocks of the Irkut terrane, Sharyzhalgai Uplift: Implications for the Neoproterozoic evolution of the Siberian Craton. *Gondwana Res.* 21 (4), 801–817.
- Urmantseva, L.N., Turkina, O.M., Larionov, A.N., 2012. Metasedimentary rocks of the Angara-Kan granulite-gneiss block (Yenisey Ridge, southwestern margin of the Siberian Craton): Provenance characteristics, deposition and age. *J. Asian Earth Sci.* 49, 7–19.
- Wakita, H., Schmitt, R.A., Rey, P., 1970. Elemental abundances of major, minor, and trace elements in Apollo 11 lunar rocks, soil and core samples, in: Proc. Apollo 11 Lunar Sci. Conf. (5–8 January, 1970, Houston), pp. 1685–1717.
- Watson, E.B., Harrison, T.M., 1983. Zircon saturation revisited: temperature and composition effects in a variety of crustal magma types. *Earth Planet. Sci. Lett.* 64 (2), 295–304.
- Whalen, J.B., Currie, K.L., Chappel, B.W., 1987. A-type granites: geochemical characteristics and petrogenesis. *Contrib. Mineral. Petrol.* 95 (4), 407–419.
- Williams, I.S., 1998. U–Th–Pb Geochronology by Ion Microprobe, in: McKibben, M.A., Shanks III, W.C., Ridley W.I. (Eds.), *Applications of Microanalytical Techniques to Understanding Mineralizing Processes*. Rev. Econ. Geol. 7, 1–35.
- Winchester, J.A., Floyd, P.A., 1977. Geochemical discrimination of different magma series and their differentiation products using immobile elements. *Chem. Geol.* 20, 325–343.
- Yanshin, A.L. (Ed.), 1983. Geological Map of Southern East Siberia and Northern Mongolian People's Republic. Scale 1:1,500,000 [in Russian]. Mingeo SSSR, Moscow.